Hydrology and Earth System Sciences Discussions

Predictions of rainfall-runoff response and soil moisture dynamics in a microscale catchment using the CREW model

H. Lee[1], E. Zehe[2], and M. Sivapalan[3]

[1]School of Environmental Systems Engineering, The University of Western Australia, 35 Stirling Highway, Crawley WA 6009, Australia
[2]Institut für Geooekologie, Universitaet Potsdam, Karl-Liebknecht-Str. 24–25, Haus 1 bzw. 12, 14 476 Golm, Potsdam, Germany
[3]Departments of Geography & Civil and Environmental Engineering, University of Illinois at Urbana-Champaign, 220 Davenport Hall, 607 S. Mathews Avenue, Urbana, IL 61801, USA

Correspondence to: H. Lee (haksu@cwr.uwa.edu.au)

EGU

Abstract

Predictions of catchment hydrology have been performed generally using either physically based, distributed models or conceptual lumped or semi-distributed models. In recognition of the disadvantages of using either of these modeling approaches, namely,
5   detailed data requirements in the case of distributed modeling, and lack of physical basis of conceptual/lumped model parameters, Reggiani et al. (1998, 1999) derived, from first principles and in a general manner, the balance equations for mass, momentum and energy at what they called the Representative Elementary Watershed (or REW) scale. However, the mass balance equations of the REW approach include mass ex-
10   change flux terms which must be defined externally before their application to real catchments. Developing physically reasonable "closure relations" for these mass exchange flux terms is a crucial pre-requisite for the success of the REW approach. As a guidance to the development of closure relations expressing mass exchange fluxes as functions of relevant state variables in a physically reasonable way, and in
15   the process effectively parameterizing the effects of sub-grid or sub-REW heterogeneity of catchment physiographic properties on these mass exchange fluxes, this paper considers four different approaches, namely the field experimental approach, a theoretical/analytical approach, a numerical approach, and a hybrid approach combining one or more of the above. Based on the concept of the scaleway (Vogel and Roth,
20   2003) and the disaggregation-aggregation approach (Viney and Sivapalan, 2004), and using the data set from Weiherbach catchment in Germany, closure relations for infiltration, exfiltration and groundwater recharge were derived analytically, or on theoretical grounds, while numerical experiments with a detailed fine-scale, distributed model, CATFLOW, were used to obtain the closure relationship for seepage outflow. The de-
25   tailed model, CATFLOW, was also used to derive REW scale pressure-saturation (i.e., water retention curve) and hydraulic conductivity-saturation relationships for the unsaturated zone. Closure relations for concentrated overland flow and saturated overland flow were derived using both theoretical arguments and simpler process models. In

addition to these, to complete the specification of the REW scale balance equations, a relationship for the saturated area fraction as a function of saturated zone depth was derived for an assumed topography on the basis of TOPMODEL assumptions. These relationships were used to complete the specification of all of the REW-scale governing
5 equations (mass and momentum balance equations, closure and geometric relations) for the Weiherbach catchment, which are then employed for constructing a numerical watershed model, named the **C**ooperative **C**ommunity **C**atchment model based on the **R**epresentative **E**lementary **W**atershed approach (CREW). CREW is then used to carry out sensitivity analyses with respect to various combinations of climate, soil, veg-
10 etation and topographies, in order to test the reasonableness of the derived closure relations in the context of the complete catchment response, including interacting processes. These sensitivity analyses demonstrated that the adopted closure relations do indeed produce mostly reasonable results, and can therefore be a good basis for more careful and rigorous search for appropriate closure relations in the future. Three tests
15 are designed to assess CREW as a large scale model for Weiherbach catchment. The first test compares CREW with distributed model CATFLOW by looking at predicted soil moisture dynamics for artificially designed initial and boundary conditions. The second test is designed to see the applicabilities of the parameter values extracted from the upscaling procedures in terms of their ability to reproduce observed hydrographs within
20 the CREW modeling framework. The final test compares simulated soil moisture time series predicted by CREW with observed ones as a way of validating the predictions of CREW. The results of these three tests, together, demonstrate that CREW could indeed be an alternative modelling framework, producing results that are consistent with those of the distributed model CATFLOW, and capable of ultimately representing
25 processes actually occurring at the larger scale in a physically sound manner.

EGU

1 Introduction

Ability to make hydrological predictions has become an essential part of sustainable management of water resources, water quality and water related natural hazards, especially in environments where climatic or human induced land use changes are under way. Catchments undergoing a transition from one state to a different state through climatic or land use changes can be considered as ungauged basins, due to the fact that under conditions of change, past measurements or gauging are poor or inadequate indicators of the future. The global, decadal initiative on Predictions in Ungagued Basins or PUB (Sivapalan et al., 2003) has been designed to address this as yet unsolved problem in hydrology. To address the problem of PUB, and in particular, to predict the effects of climatic and land use changes, it is increasingly necessary to develop hydrological models that are based on a deeper level of process understanding rather than merely rely on calibrations carried out with past observations. For hydrological predictions in meso-scale catchments, the usual practice is to use so-called conceptual models, which can be lumped or quasi-distributed due to their efficiency in terms of data requirements and computational costs, traits that put them at a considerable advantage compared to physically based, fully distributed models, notwithstanding the sound theoretical basis of the latter-type models. Parameters used in lumped or quasi-distributed conceptual models often have very little physical meaning in the traditional sense, due to the lack of a physically-based theory at the catchment scale, and consequently these parameters cannot be estimated unambiguously in the field or from field data. Therefore, conceptual models will be inadequate to address PUB problems in an efficient or physically sound manner. To deal with the PUB problem, the chosen model must be flexible enough to incorporate new findings about processes in changed environments and new ways of capturing them in models. In addition, parameters of the model must be capable of being estimated from field data and of reflecting likely environmental changes, and their meanings must be sound enough on physical grounds. In order to make better predictions and reduce predictive uncertainties, the chosen model

Hydrological modeling with the REW approach

H. Lee et al.

Title Page

Abstract	Introduction
Conclusions	References
Tables	Figures

⏮   ⏭

◀   ▶

Back   Close

Full Screen / Esc

Printer-friendly Version

Interactive Discussion

EGU

must have a holistic model structure that incorporates changes in the environment in a consistent manner so as to reduce model structure uncertainties.

Recently, Reggiani et al. (1998, 1999) proposed a new hydrological modeling framework based on balance equations for mass, force and energy, derived directly at the scale of what they called the Representative Elementary Watershed (REW). The REW approach presents, potentially, a novel framework for developing hydrological models directly at the catchment scale, in a physically based and also physically meaningful manner. The REW approach offers several advantages over traditional (lumped or quasi-distributed) conceptual models, and over the current generation of physically based, fully distributed (grid based) models. Firstly, the governing equations derived as part of the REW approach are applicable directly at the catchment scale, as opposed to at the point or REV scale, as in the current generation of distributed models. Therefore, models based on the the REW scale balance equations remain modest in terms of both their computational burden and their input and parameter requirements. Secondly, the REW scale balance equations have been derived in a comprehensive manner for the whole catchment or REW, as opposed to being derived separately for different processes, as is the case with many traditional distributed models. Special care has been taken to respect not only the individual component processes, but also the various process interactions amongst parts of the REW. This enhances the holistic nature of the REW approach for characterizing overall catchment responses. Thirdly, by being general and not tied to specific process formulations, e.g., about how to describe mass and/or momentum exchanges at the REW scale, as is the case with traditional distributed models that rely on point or REV scale formulations, e.g., Darcy's law, the REW approach is much more flexible in the sense of a modelling framework. Hence, the REW approach can easily benefit from further advances in process understanding and process descriptions emerging from new field experiments carried out at the hillslope or REW/catchment scale.

The "heart" of the REW approach is the set of coupled mass and force balance equations for "different zones" within an REW, such as the unsaturated zone, the saturated

zone and the channel zone. However, mass fluxes between these different zones are generally unknown, with the result that there are many more unknowns than there are balance equations, making the set of balance equations indeterminate. This is called the "closure problem". In this context, closure means essentially the development of
5 physically reasonable process formulation for the various mass exchange fluxes that incorporate the effects of sub-REW scale spatial heterogeneities, and expressed in terms of selected REW scale state variables and catchment characteristics. A related problem is the derivation of REW scale constitutive relations that relate one or more state variables amongst themselves, e.g. REW scale capillary pressure vs. saturation
10 and hydraulic conductivity vs saturation relationships in the unsaturated zone, again incorporating the effects of sub-REW scale heterogeneities.

To a certain extent, the closure relations represent an upscaling of process descriptions available at the point or REV scale, towards physically reasonable process parameterizations appropriate to the REW scale. In fact, they could be much more than this,
15 and could represent processes that occur at the larger (e.g., REW) scale, and requiring descriptions that transcend familiar small scale ones, in which case simple upscaling approaches may not be adequate. In either case, theory alone, of the sort used in the derivation of the REW scale balance equations and constitutive theory, i.e., Newton's laws of motion and the 2nd law of thermodynamics, is not sufficient to generate
20 these. Ideally, they will have to be estimated from experiments in the field, or through appropriate integration of assumed, measured or simulated realistic patterns of subgrid, or sub-REW, heterogeneity. Indeed, the closure relations are the best mechanism to ground the REW theory to reality, through physically realistic and reasonable descriptions of actual hydrological processes and their underlying physical mechanisms,
25 expressed in terms of parameterizations involving landscape and climatic properties. Therefore, they are also intimately connected to the issue of estimation model parameters.

It is therefore clear that to make progress in turning the REW approach into a viable new model blueprint, we need to develop a consistent upscaling framework to develop

EGU

closure relations and assess the related parameters/ constitutive relations that are valid at the REW scale (Beven, 2002; Reggiani and Schellekens, 2003). The chief focus of this paper is on the derivation and assessment of various closure relations and constitutive relations for a micro-scale catchment located in south-west Germany. Our main objective is to explore alternative approaches currently available, and being used, for the required upscaling, and to report on the progress made so far in developing closure relations using these methods. We will then present the resulting complete set of coupled balance equations for mass and momentum, and the associated geometric relations. Subsequently, we will present sensitivity analysis with the resulting complete REW-scale model to explore and to confirm that the adopted closure relations do behave in a physically reasonable manner in response to realistic climatic inputs (rainfall and potential evaporation) in an actual catchment. We then compare the predictions of a fully distributed (grid scale) model with those of the REW scale model by looking at temporal soil moisture patterns generated by both models. Finally, the resulting REW-scale model is used to illustrate the applicability of catchment scale parameter values obtained for the Weiherbach catchment during the upscaling procedure.

The material in the paper is organized as follows. We begin with a summary of the REW scale balance equations of mass and momentum developed by Reggiani et al. (1998, 1999). This is followed by a discussion of the closure problem as it relates to the REW approach, and a review of upscaling methods applicable for the derivation of closure relations at the catchment scale. We then illustrate the application of these methods for the derivation of closure relations for a number of mass exchange fluxes in an actual catchment. This completes the specification of the mass and momentum balance equations for the catchment in question. A numerical model of the resulting set of coupled equations is then utilized to perform sensitivity analyses designed to test the physical reasonableness of the developed closure relations within the REW modeling framework. We then conduct a comparison of grid scale, fully distributed, physically based model, CATFLOW, with the REW-scale, lumped, physically based model. Finally, we apply the resulting model to the Weiherbach catchment to demonstrate the

EGU

applicability of catchment scale parameter values estimated prior to model application.

2 The REW-approach and the study area

2.1 The REW approach as foundation for meso-scale models

An REW is taken as the smallest resolvable spatial unit of a meso-scale watershed,
5 and is composed of five zones: unsaturated zone (u-zone), saturated zone (s-zone), concentrated overland flow zone (c-zone), saturated overland flow zone (o-zone), and channel zone (r-zone). These are delineated based on known physical characteristics of typical watersheds, and on characteristic time scales that are typical of various hydrological processes (Reggiani et al., 1998). The mass, energy and momentum bal-
10 ances within the individual zones of the REW are described using a coupled set of ordinary differential equations, derived from thermodynamic principles, by means of averaging. Figure 1 presents the schematic of a typical watershed that is discretized into three REWs based on the geometry of channel network, and Fig. 1b illustrates the sub-regions making up the REW, and the mass exchange fluxes between different
15 sub-regions of each REW, and those between different REWs. A simpler set of REW-scale balance equations of mass and momentum applicable to these REWs and their sub-regions, from those first derived by Reggiani et al. (1998, 1999) is used in the rest of this paper. These are presented in Eqs. (1) to (11) below. For further details regarding their derivation and the meaning of the variables, the reader is referred to Reggiani
20 et al. (1998, 1999, 2000), and the nomenclature given at the end of the paper.

$$\underbrace{\frac{d}{dt}(\varepsilon y^s \omega^s)}_{\text{storage}} = \underbrace{e^{so}}_{\text{seepage}} + \underbrace{e^{su}}_{\substack{\text{exchag.with} \\ \text{unsat.zone}}} + \underbrace{e^{sr}}_{\text{sat.zone--river exchange}} + \underbrace{\sum_l e^{sA}_l + e^{sA}_{ext}}_{\text{exchange across mantle segments}} \tag{1}$$

Hydrological modeling with the REW approach

H. Lee et al.

⏮ | ⏭

◀ | ▶

Back | Close

Full Screen / Esc

Printer-friendly Version

Interactive Discussion

EGU

$$\underbrace{\frac{d}{dt}(\varepsilon y^u \omega^u s^u)}_{\text{storage}} = \underbrace{e^{uc}}_{\text{infiltration}} + \underbrace{e^{us}}_{\substack{\text{exchag.with} \\ \text{sat.zone}}} + \underbrace{e^u_{wg}}_{\text{evaporation}} + \underbrace{\sum_l e^{uA}_l + e^{uA}_{ext}}_{\text{exchange across mantle segments}} \tag{2}$$

$$\underbrace{\frac{d}{dt}(y^c \omega^c)}_{storage} = \underbrace{e^{cu}}_{\text{infiltration into unsat. zone}} + \underbrace{e^{co}}_{\text{flow to sat. overl. flow}} + \underbrace{e^{ctop}}_{\text{rainfallorevaporation}} \tag{3}$$

$$\underbrace{\frac{d}{dt}(y^o \omega^o)}_{\text{storage}} = \underbrace{e^{or}}_{\text{lat. channel inflow}} + \underbrace{e^{os}}_{\text{seepage}} + \underbrace{e^{oc}}_{\text{inflow from conc. overl. flow}} + \underbrace{e^{otop}}_{\text{rainfallorevaporation}} \tag{4}$$

$$\underbrace{\frac{d}{dt}(m^r \xi^r)}_{\text{storage}} = \underbrace{e^{ro}}_{\text{lateral inflow}} + \underbrace{e^{rs}}_{\text{channel−sat. zone exch.}} + \underbrace{\sum_l e^{rA}_l + e^{rA}_{ext}}_{\text{inflow, outflow}} + \underbrace{e^{rtop}}_{\text{rainfall or evaporation}} \tag{5}$$

$$\underbrace{\pm \sum_l A^{sA}_{l,\lambda} \left[-p^s + \rho \left(\phi^{sA}_l - \phi^s \right) \right]}_{\text{inter−REW driving force}} + \underbrace{\pm A^{sA}_{ext,\lambda} \left[-p^s + \rho \left(\phi^{sA}_{ext} - \phi^s \right) \right]}_{\text{force acting on the external boundary}} + \underbrace{\pm A^{sbot}_\lambda \left[-p^s + \rho \left(\phi^{s\,bot} - \phi^s \right) \right]}_{\text{force at the bottom boundary}}$$
$$= \underbrace{-R^s v^s_\lambda}_{\text{resistance to flow}} \quad ; \lambda = x, y \tag{6}$$

5

$$\underbrace{\pm \sum_l A^{uA}_{l,\lambda} \left[-p^u + \rho \left(\phi^{uA}_l - \phi^u \right) \right]}_{\text{inter−REW driving force}} + \underbrace{\pm A^{uA}_{ext,\lambda} \left[-p^u + \rho \left(\phi^{uA}_{ext} - \phi^u \right) \right]}_{\text{force acting on the external boundary}} = \underbrace{-R^u v^u_\lambda}_{\text{resistance to flow}} \quad ; \lambda = x, y \tag{7}$$

$$\underbrace{\left[-p^u + \rho \left(\phi^{uc} - \phi^u \right) \right] \varepsilon \omega^u}_{\text{force top}} - \underbrace{\rho \varepsilon s^u y^u \omega^u g}_{\text{gravity}} = \underbrace{-R^u v^u_z}_{\text{resistance force}} \tag{8}$$

Hydrological modeling with the REW approach

H. Lee et al.

Title Page

Abstract	Introduction
Conclusions	References
Tables	Figures

◄◄	►►
◄	►
Back	Close

Full Screen / Esc

Printer-friendly Version

Interactive Discussion

EGU

$$\underbrace{(\rho y^c \omega^c) \frac{dv^c}{dt}}_{\text{inertial term}} - \underbrace{\rho y^c \omega^c g \sin \gamma^c}_{\text{gravity}} = \underbrace{-U^c v^c |v^c|}_{\text{resistance to flow}} \tag{9}$$

$$\underbrace{(\rho y^o \omega^o) \frac{dv^o}{dt}}_{\text{inertial term}} - \underbrace{\rho y^o \omega^o g \sin \gamma^o}_{\text{gravity}} = \underbrace{-U^o v^o |v^o|}_{\text{resistance to flow}} \tag{10}$$

$$\underbrace{(\rho m^r \xi^r) \frac{dv^r}{dt}}_{\text{inertial term}} = \underbrace{\rho g m^r \xi^r \sin \gamma^r}_{\text{gravitational force}} - \underbrace{U^r v^r |v^r|}_{\text{Chezy resistance}}$$

$$+ \underbrace{\pm \sum_l A_l^{rA} \cos \delta_l \left[-p^r + \rho \left(\phi_l^{rA} - \phi^r \right) \right]}_{\text{pressure forces exchanged among REWs}} + \underbrace{A_{\text{ext}}^{rA} \left[-p^r + \rho \left(\phi_{\text{ext}}^{rA} - \phi^r \right) \right]}_{\text{pressure force at watershed outlet}} \tag{11}$$

where ε is porosity, y^i ($i=u,s,c,o,r$) is the average vertical thickness of the i subregion,

ω^i ($i=u,s,c,o,r$) is the time averaged surface area fraction of the i subregion, s^u is the saturation degree of the unsaturated zone, m^r is the channel cross sectional area, ξ^r is the drainage density, e^{ij} (i or $j=u,s,c,o,r$) the rate of water mass exchange between the i and j subregions, e_{wg}^u is the rate of evapotranspiration from the unsaturated zone, e_l^{jA} ($j=u,s,r$) is the rate of water mass exchange from the j subregion across the lth

mantle segment, e_{ext}^{jA} ($j=u,s,r$) is the water mass exchange from the j subregion across the external watershed boundary, A_l^{jA} and A_{ext}^{jA} ($j=u,s,r$) are the mantle surface with horizontal normal delimiting the REW externally at the j subregion with the lth mantle segment and the external watershed boundary, respectively, $A^{s\,\text{bot}}$ is the mantle surface corresponding to the bottom part of the saturated zone, p^i ($i=u,s,r$) is the pressure of

the i subregion, ρ is water mass density, ϕ^i, $\phi^{s\,\text{bot}}$, ϕ_l^{iA}, and ϕ_{ext}^{iA} ($i=u,s,r$) are the gravitational potential at the i subregion, at the bottom part of the saturated zone, at the interface of the i subregion and lth mantle segment, and at the interface of the i

subregion and the external watershed boundary, respectively, v^i ($i=u,s,c,o,r$) is the water velocity within i subregion, v_z^u is the vertical water velocity within the unsaturated zone, g is gravitational acceleration, R^i ($i=u,s$) is the first order friction term of the i subregion, U^i ($i=c,o,r$) is the second order friction term of the i subregion, γ^i ($i=c,o,r$)

5 is the slope angle of the i subregion flow plane with respect to the horizontal plane, and δ_l is the local angle between the reach of the lth REW and the reach of the REW of interest.

To summarize, Eqs. (1) to (5) represent, respectively, mass balance of the saturated zone (s-zone), the unsaturated zone (u-zone), the concentrated overland flow zone

10 (c-zone), the saturated overland flow zone (o-zone), and the channel reach (r-zone). Equations (6) to (11) represent momentum balance of the saturated zone, unsaturated zone in the horizontal direction, unsaturated zone in the vertical direction, concentrated overland flow zone, saturated overland flow zone and the channel reach.

2.2 The closure problem

15 The e^{ij} terms in the mass balance equations (1) to (5), also shown in Fig. 1b, represent mass exchange fluxes between the i and j sub-regions such as infiltration, bare soil evaporation and transpiration by root uptake, groundwater recharge/capillary rise, saturated and concentrated overland flow, seepage outflow, and channel flow. These fluxes are generally unknown, and must be externally specified. Therefore, in order to

20 close the set of equations, i.e., to make the number of equations equal to the number of unknowns, the exchange fluxes must be expressed in terms of other resolved variables, namely the state variables relating to the sub-regions between which the mass fluxes are being exchanged – we call this the closure problem. The balance equations must be closed in such a way that the adopted closure relations encapsulate what is

25 presently known about the actual processes and mechanisms governing these fluxes. They will also be expected to incorporate the effects of sub-grid heterogeneities of climate, soils, topography and vegetation, as expressed through a number of exchange

coefficients, which will appear as parameters in the adopted closure relations. In this way, the REW approach parameterizes the effects of variabilities occurring at scales smaller than the REW, and explicitly resolves variabilities occurring over scales larger than the REW.

Our approach for developing closure relations builds on the disaggregation-aggregation approach outlined by Sivapalan (1993) and Viney and Sivapalan (2004), and was significantly influenced by the scaleway concept of Vogel and Roth (2003). The latter argues that in environmental modelling one has to deal with "texture", which is not explicitly resolved, the effects of which are parameterized using a continuum formulation of the relevant processes or exchange fluxes, and "structure", which is explicitly resolved. For a standard distributed hydrological model, the soil matrix is the texture and well described by Richards' equation and appropriate soil hydraulic functions that represent the topology and connectivity of the pore spaces. Structures may be the spatial patterns of soils, including soil layering and possible preferential pathways. Moving on to the REW scale, it can be expected that the spatial patterns of soils and preferential pathways will affect mass exchange fluxes, and will in turn become the "texture" at the REW scale. In this sense, it is essential to assess REW-scale textural properties and associated parameters, which embed the effects of the sub-scale structures on the mass exchange fluxes at the REW scale.

The concept of "the scaleway" proposed by Vogel and Roth (2003) can provide some guidance towards dealing with multi-scale heterogeneities with given structures, textures, material properties, and appropriate process models, to come up with appropriate closure relations as well effective material properties at the next larger scale. Here, we define a few terms for the the sake of clarity, which is taken from Vogel and Roth (2003). The scale of observation is the linear extent of the entire investigated region. Structure is the one that is composed of form elements comparable in size with the scale of observation, while the textural elements are very much smaller. To derive closure relations at the given study area, it is a prerequisite to recognize and represent explicitly different structures, textures, and material properties at the given ob-

Hydrological modeling with the REW approach

H. Lee et al.

Title Page

Abstract	Introduction
Conclusions	References
Tables	Figures

◀ ▶

◀ ▶

Back | Close

Full Screen / Esc

Printer-friendly Version

Interactive Discussion

EGU

servational scale to come up with appropriate closure relations applicable to the given study area. Depending on different types of sptial heterogeneities across observational scales, the type of structural organization emergent at the larger scale is also different, e.g., macroscopic homogeneity, discrete hierarchy, continuous hierarchy, and fractals as shown by Vogel and Roth (2003). This indicates information transfer from the lower scale to the next higher scale through effective parameters. Besides, this describes the dependence of the parameter values to the given observational scale, which also gives rise to the problem of parameter estimation at the next larger scale. Therefore, to assess the appropriateness of developed closure relations, it is good practice to test the hydrological model incorporated with developed closure relations with parameter values obtained from the procedure of development of closure relations.

Within this study we will assume that the hydrological micro-scale, i.e. the scale of small experimental catchments, is a key scale for the derivation of physically sound closure relations because:

- the micro-scale is small enough so that we can gain a reasonable understanding of how spatial patterns of soils and preferential pathways affect various mass exchange fluxes through the use of detailed field observations and distributed models; and

- the micro-scale is large enough so that we can set up a model based on the REW-approach to simulate average or typical hydrological dynamics in this region and to perform comparative simulations.

These assumptions provide the main justification for using the micro-scale experimental catchment, Weiherbach, in south-west Germany, for the derivation of the required closure relations.

2.3 Study area

As mentioned above, Weiherbach catchment was selected as the study area for developing closure relations for various mass exchange fluxes. The Weiherbach is a

Hydrological modeling with the REW approach

H. Lee et al.

Title Page

Abstract | Introduction

Conclusions | References

Tables | Figures

◄◄ | ►►

◄ | ►

Back | Close

Full Screen / Esc

Printer-friendly Version

Interactive Discussion

EGU

rural catchment of 3.6 km^2 size situated in a Loess area in the south-west of Germany. Geologically, it consists of Keuper and Loess layers up to 15 m thick. The climate is semi-humid with an average annual precipitation of 750 to 800 mm/yr, average annual runoff of 150 mm/yr and annual potential evapotranspiration of 775 mm/yr (Zehe et al., 2001). More than 95% of the catchment area is used for cultivation of agricultural crops or pasture, 4% is forested and 1% is paved area. Most of the Weiherbach hillslopes exhibit a typical Loess catena with moist but drained Colluvisols located at the foothills, and drier calcareous Regosols located at the hilltops and mid-slope regions. Figure 2 gives an overview of the observational network of the Weiherbach catchment. Rainfall inputs were measured in a total of 6 rain gages, and streamflows were monitored at a temporal resolution of 6 min. The catchment area up to the stream gauge is 3.6 km^2. Soil moisture was measured at up to 61 locations at weekly intervals using two-rod TDR equipment that integrates over the upper 15 cm, upper 30 cm, upper 45 cm and upper 60 cm of the soil. The soil hydraulic properties of typical Weiherbach soils, after van Genuchten (1980) and Mualem (1976), were measured in the laboratory using undisturbed soil samples taken along transects at several hillslopes, with up to 200 samples per slope (Table 1, Schäfer, 1999).

The Weiherbach catchment offers considerable advantages for the development of closure relations. Firstly, it has been maintained as a significant experimental catchment over the past many years. There is a wealth of information regarding the geology and soil properties, and field experimentation has generated a wealth of measurements of various water fluxes and internal soil state variables, such as soil moisture and groundwater table profiles, in space and time. Secondly, a detailed physically based model (using the finite difference scheme), CATFLOW (Maurer, 1997; Zehe et al., 2001; Zehe and Blöschl, 2004), has been developed and successfully verified using the detailed data collected during the field experiments. In this paper, this model is used for the development of the closure relations relating to seepage (subsurface) outflow, and the pressure-saturation and conductivity-saturation relationships.

3   Derivation of closure relations and the CREW model

3.1   Different approaches for assessing closure relations

In this section, we review the upscaling methods that are currently available to develop closure relations for mass exchange fluxes. We classify these upscaling methods into four categories: field experiments, theoretical/analytical derivations, numerical experiments, and hybrid approaches.

3.1.1   Assessing closure relations based on field experiments

The field experimental approach seeks to find closure relations from the analysis of data obtained in the field, either in a routine manner or through focused intensive field experiments. Empirical closure relations based on field observations may be the best candidates for the REW scale closure relations, because they best represent the intrinsic natural variability occurring within the study catchment. These include nonlinear and threshold behavior commonly exhibited in many catchments, which are hard to represent using current small-scale theories. Unfortunately, in most cases, field monitoring of catchments is limited to rainfall, runoff, and potential evaporation, which are not sufficient to derive closure relations. At the minimum, the development of closure relations requires measurements of internal state variables in different sub-regions of the catchment system. Unfortunately, currently there are no measurement techniques available that allow observations of internal states and subsurface structures for scales larger than the plot- or small field scale (Schulz et al., 2006). While they have been monitored as part of some focused field experiments around the world, such as soil moisture measurement at the Tarrawarra catchment in southern Victoria, Australia (Western and Grayson, 1998), and the Weiherbach catchment, and at over 600 stations from around the globe (Robock et al., 2000), mostly by employing a distributed network of point measurements, the corresponding data from these field experiments alone is not sufficient for derivation of closure relations. The work of Duffy (1996) at the Shale

Hills catchment in central Pennsylvania is an exception to this trend, and showed that closure relations, notably the storage-discharge relationship relating to shallow sub-surface flow, can be derived on the basis of carefully conducted field experiments, in combination with numerical modelling.

3.1.2 Analytical approach to the derivation of closure relations

In the theoretical/analytical approach, the emphasis is on deriving closure relations through analytical integration or upscaling of small-scale physically based equations through mathematical manipulation. A widely used approach is the derivation of effective parameters by means of coarse graining, as suggested by Dagan (1989), Attinger (2003) and Lunati et al. (2002), which is based on assumptions on the probability distributions of key parameters, e.g. the hydraulic conductivity. While this is a useful approach for groundwater, it is too simple for the unsaturated zone and surface processes. This is firstly because the variability of these processes is controlled by the nonlinear interaction of several structures/patterns in a catchment e.g. vegetation, soil hydraulic properties, macroporosity and topography, where the state of the catchment determines which of these patterns is the dominant one (Zehe and Blöschl, 2004). And secondly, the spatial characteristics of these patterns, i.e. the correlation structure and more importantly their connectivity may not be captured with simple analytical functions (Blöschl and Zehe, 2005). However, in some cases this approach has the advantage that the resulting closure relations, as well as the consequent REW scale parameters, retain some or most of their traditional meaning, and therefore there is a chance that they can be estimated by referring back to a mapping of landscape and/or climatic properties.

3.1.3 Numerical simulation approach to the derivation of closure relations

The numerical simulation approach seeks to derive closure relations based on the comprehensive simulated datasets that can be generated through the application of

HESSD

3, 1667–1743, 2006

Hydrological modeling with the REW approach

H. Lee et al.

Title Page

Abstract | Introduction

Conclusions | References

Tables | Figures

◄ | ►

◄ | ►

Back | Close

Full Screen / Esc

Printer-friendly Version

Interactive Discussion

EGU

detailed, distributed physically-based hydrological models that are based on small-scale physical theories, under well defined boundary conditions. In contrast to the analytical approach, these models may account explicitly for all the patterns of vegetation, soil properties, macropores and topography, and their nonlinear interactions, that may be controlling the surface and subsurface flows. Closure relations maybe derived from numerical model output by averaging the state variables and parameter fields to the catchment or REW scale and postulating parametric relations. However, the main problem with this approach is that the patterns of vegetation, soil properties (soil hydraulic functions), macropores, and the small scale heterogeneity and the small/larger scale connectivity of preferred pathways are simply unknown for most catchments in the world. So one either has to work with assumptions or has to focus on well instrumented research catchments, as we do in the present study. In such cases the numerical simulation approach can nevertheless be a good starting point for developing closure relations at the catchment scale (Zehe et al., 2005a; Kees et al., 2002, 2004) that are accurate to first order. Zehe et al. (2005a) and Kees et al. (2004) presented examples of the development of closure relations for a hillslope scale water balance model with a transient numerical solution of continuum-scale model.

3.1.4 Hybrid approaches for assessing closure relations

In the present study we also follow the hybrid approach, which is a combination of any of the above methods presented above. Viney and Sivapalan (2004), following Robinson and Sivapalan (1995), derived closure relations for catchment scale infiltration capacity as a function of the cumulative volume of infiltrated water on the basis on numerical experiments and catchment response data. They tested the effects of different storms as well as different topographies on this relationship, and through these sensitivity analyses parameterized the relationship in terms of storm duration, storm depth, temporal pattern and catchment topography. This led to an acceptable empirical closure relation for infiltration rate that could be embedded within a large-scale catchment model.

EGU

In a similar way, we apply a number of these methods to develop closure relations for crucial mass exchange fluxes appearing in the REW scale balance equations; these derivations are presented in Sects. 3.2.1 to 3.2.6. Supplementary parametrizations such as a geometric relationship for saturated surface area, the REW scale water-retention curve, and the hydraulic conductivity versus saturation relationship, are de-rived in Sects. 3.3.1 to 3.3.3. In Sect. 3.4 the developed closure relations are combined, with the original balance equations, yielding a set of equations which form the basis of the CREW model.

3.2 Closure relations for mass exchange fluxes

3.2.1 Infiltration e^{uc}

For the infiltration process during rainfall events we directly use the results of Rogers (1992) who developed an areal average infiltration capacity model based on the stan-dard Green-Ampt equation. He assumed that only saturated hydraulic conductivity is spatially variable, and that it follows a log-normal distribution. All other soil parameters were assumed constant, with the justification that saturated hydraulic conductivity is much more variable than the other parameters and has a greater impact on infiltration (Bresler and Dagan, 1983). The resulting infiltration capacity equation has the following form:

$$\overline{f*} = \overline{K_s}\left[1 + \alpha^{uc}\frac{|\Psi_f|(\theta_s - \theta_i)}{\bar{F}}\right] \tag{12}$$

where $\overline{f*}$ is spatially averaged infiltration capacity, $\overline{K_s}$ is mean saturated hydraulic con-ductivity, $|\Psi_f|$ is soil's matric potential head at the wetting front, θ_s is saturated soil moisture content, θ_i is initial soil moisture content, $\bar{F}$ is spatially averaged cumulative volume of infiltration and α^{uc} is a parameter related to the variability of hydraulic con-ductivity. To adapt Eq. (12) within the REW modeling framework, we need to find a match between state variables in Eq. (12) and those of the REW approach. Since $\bar{F}$

corresponds to infiltrated water depth into the unsaturated zone, it was replaced by $s^u y^u$, where s^u is degree of saturation in the unsaturated zone and y^u is average thickness of the unsaturated zone along the vertical. $|\Psi_f|$ and $\theta_s - \theta$ are replaced by $|\Psi|$ and $(1-s^u)\varepsilon^u$, respectively, where $|\Psi|$ is the soil's matric potential head (which is a function of saturation degree in the unsaturated zone) and ε^u is soil porosity in the unsaturated zone. The resulting form of the infiltration capacity equation is:

$$\overline{f^*} = \overline{K_s}\left[1 + \alpha^{uc}\frac{|\Psi|\left(1 - s^u\right)\varepsilon^u}{s^u y^u} \right] \tag{13}$$

where α^{uc} embeds within it the effects of not only the spatial variability of soils, but also of the space-time variability of the wetting front position during the infiltration process. The infiltration capacity Eq. (13), which is based on and resembles the standard Green-Ampt infiltration equation, still has much room for improvement to account for new findings from field experiments and to provide improved predictions of ponding time, and the effect of rainfall heterogeneities on the infiltration process.

Finally, as in Reggiani et al. (2000), the actual infiltration flux (e^{uc}) during rainfall events can be expressed as:

$$e^{uc} = \min\left[i\varpi^u, \ \overline{f^*}\varpi^u \right] \tag{14}$$

where i is rainfall intensity and ϖ^u is the surface area fraction occupied by the unsaturated zone.

3.2.2 Bare soil evaporation and transpiration by root uptake

Closure relations for bare soil evaporation and transpiration by root uptake were derived analytically based on the exfiltration capacity model of Eagleson (1978b, c), assuming that the soil hydraulic conductivity is spatially variable and follows a log-normal distri-

bution. The resulting closure relations have the following final form:

$$e_{wg}^u = \min\left[\left(e_p + Mk_v\overline{e_p}\right)\varpi^u, \;\; \overline{f_{ET}^*}\varpi^u\right] \tag{15}$$

$$\overline{f_{ET}^*} = \alpha_{wg}^u \frac{\overline{K_s}}{(1-s^u)\,y^u} \frac{(s^u)^{2+d}\,\varepsilon^u\,|\Psi_b|}{m} \tag{16}$$

where e_p is potential evaporation rate from the bare soil surface, M is the vegetated
fraction of land surface, i.e., canopy density, k_v is the ratio of potential rates of transpi-
ration and soil surface evaporation, $\overline{e_p}$ is the long-term (time averaged) rate of potential
(soil surface) evaporation, $\overline{f_{ET}^*}$ is the spatially averaged combined exfiltration capacity
due to bare soil evaporation and transpiration by root uptake, m is pore size distribution
index, c is pore disconnectedness index, ε^u is soil porosity in the unsaturated zone,
d is diffusivity index, $|\Psi_b|$ is the bubbling pressure head, and α_{wg}^u is a parameter re-
lated to variability of saturated hydraulic conductivity and exfiltration diffusivity. The full
derivation of these equations is presented in detail in Appendix A.

3.2.3 Groundwater recharge/capillary rise

Groundwater recharge/capillary rise, in general, refers to the mass exchanges between
the unsaturated zone and the saturated zone that lies below it. Depending on its dom-
inant direction it can take on different meanings. It will be called net recharge if the net
water flow is vertically downward into the saturated zone, while it will be termed capil-
lary rise if the net flow is vertically upward into the unsaturated zone. The direction of
flow at any time is governed by the status of momentum balance within the unsaturated
zone, expressed through the resulting unsaturated zone vertical velocity v_z^u. In this pa-
per, as a first step, we develop somewhat simple closure relationship for the recharge
flux/capillary rise of the following form:

$$e^{us} = \alpha^{us}\varpi^u v_z^u \tag{17}$$

where α^{us} is considered as a constant of proportionality linking the average vertical velocity with the entire unsaturated zone and the recharge/capillary rise at the bottom, which is a boundary flux. The form of this closure relation, Eq. (17), has a similar form to that of Reggiani et al. (2000). Here it should be pointed out that the improvement of this closure relation lies not only in the way of parameterizing e^{us} but also in the way of relating v_z^u to both relevant state variables and material properties by adopting appropriate expressions for the non-equilibrium part of the momentum exchange terms. At the moment, we are adopting first-order Taylor series expansion for deriving v_z^u which leads to the result that appears in Eq. (8) and similar to the equation adopted by Reggiani et al. (2000). However, in locations where subsurface flow is highly dominated by fast flow processes due to the presence of a highly organized network of macropores or connected flow pathways, a higher order Taylor series expansion would be more suitable to describe the non-equilibrium part of the momentum exchange terms. This will lead to a different form for v_z^u from the one shown in Eq. (8).

3.2.4 Saturated and concentrated overland flow

A closure relation for saturated overland flow was obtained by adopting the numerical simulation approach, and using the steady-state solution for the kinematic wave equation governing overland flow, improved to consider the effect of field capacity on water flow through soil media (Ichikawa and Shiiba, 2002). Based on the results of numerical simulations applied to the Weiherbach catchment, several functional relationships between saturated overland flow and the state variables relating to overland flow were explored. It was found from these simulations that e^{ro} is linearly proportional to the product of the average flow depth of the saturated overland flow zone (y^o) and the average velocity of overland flow (v^o), i.e., $e^{ro}=\alpha_1^{ro}y^o v^o$, where α_1^{ro} is an exchange coefficient that remained to be estimated. A further investigation was carried out to examine the dependence of α_1^{ro} on the total length of channels within the REW. For this investigation, the Weiherbach catchment was divided into 39 basin groups, and these were subjected to rainfall events with intensities ranging from 0.1 to 40 mm/h. Figure 3

EGU

presents the results describing the dependence of α_1^{ro} on total channel length. The relationship between α_1^{ro} and channel length does show a small dependence on rainfall intensity, as expressed through the scatter, which increases as the size of the REW increases. Generally, however, a strong linear dependence on total channel length can

5 be seen in Fig. 3. On the basis of these results, the following closure relation is adopted for saturated overland flow:

$$e^{ro} = \alpha^{ro}\xi^r y^o v^o \tag{18}$$

where ξ^r is defined as the length of channels per unit surface area, which can be considered as equivalent to the catchment's drainage density, and α^{ro} is now a dimen-

10 sionless constant of proportionality.

It is assumed that overland flow over the concentrated overland flow zone, generated by the infiltration excess mechanism, could be closed with a function of the same form as that of saturated overland flow. Therefore, the suggested closure relation is:

$$e^{oc} = \alpha^{oc}\xi^r y^c v^c \tag{19}$$

15 where ξ^r is the length of the channel reach per unit surface area, or drainage density. In both closure relations for saturated and concentrated overlad flow, we should take more care about the way to describe velocity terms, v^c and v^o, in such a way that the velocities estimated from Eqs. (9) and (10), with carefully chosen surface roughnesses and surface slopes at the REW scale, should be compatible with the corresponding

20 averages estimated from predictions of the distributed model.

3.2.5 Seepage outflow

The closure relation for seepage outflow was obtained by using the numerical simulation approach. For this the physically based distributed model CATFLOW (Maurer, 1997; Zehe et al., 2001) was used, and applied to the Weiherbach catchment in Ger-

25 many. CATFLOW is capable of simulating continuous space-time dynamics of water

EGU

flow and transport of solutes in the upper soil layer of small rural catchments, including channel network and vegetation cover, on event and seasonal time scales, over the three dimensional spatial domain. CATFLOW utilizes the 2-D Richards equation and 2-D transport equation to model water and solute dynamics in the soil matrix respectively,

5 Penman-Monteith equation for evapotranspiration, and 1-D Saint-Venant equation for runoff from hillslopes, as well as flow in the drainage network. CATFLOW is also capable of handling the presence of macropores (Zehe et al., 2001), with a simplified effective parameter approach. If water saturation in macroporous soil exceeds field capacity, the bulk hydraulic conductivity at this point is assumed to increase linearly

10 up to a maximum value at saturation, which is determined by the macroporosity factor f_M. The macroporosity factor is the ratio of the water flow rate in the macropores, in a model element of area A, with the saturated water flow rate in the soil matrix. It is therefore a characteristic soil property reflecting the maximum influence of active preferential pathways on the soil water movement. CATFLOW has been verified on the

15 Weiherbach catchment using tracers and rainfall-runoff data, with good success. We are, therefore, confident that the model is able to reproduce well the internal mechanisms of water movement, storage, runoff generation and evapotranspiration, including the substantial space-time variability.

As a first step, a hillslope with soil catena and a spatial pattern of macroporosity typical for the Weiherbach catchment was chosen as the spatial domain (Zehe and

20 Blöschl, 2004). The hillslope was discretized into 21 nodes horizontally and 21 layers vertically. In the upper 80% of the hillslope a Loess soil is located; the lower 20% consist of Colluviosol. The dependence of soil water potential and unsaturated hydraulic conductivity on soil moisture saturation is expressed in terms of the van Genuchten

25 (1980) and Mualem (1976) formulations (Table 1) given below:

$$s = \frac{\theta - \theta_r}{\theta_s - \theta_r} = \left[\frac{1}{1 + \left(\overline{\alpha} \, |\psi| \right)^n} \right]^{\frac{n-1}{n}} \qquad (20)$$

Full Screen / Esc

Printer-friendly Version

Interactive Discussion

$$K = K_s s^{1/2} \left[1 - \left[1 - s^{\frac{n}{n-1}} \right]^{\frac{n-1}{n}} \right]^2 \qquad (21)$$

Vertical soil depth is set at 2 m. Following the suggestions of Zehe et al. (2001) a spatially variable macro-porosity factor was assigned along the length of the hillslope profile, with fixed relative portions $0.6f_M$ for the upper 70%, $1.1f_M$ for the 70 to 85%,

5 and $1.5f_M$ for the 85% to 100% part of the hillslope. The average macro-porosity factor was taken to be $f_M=2.1$. To check the possible influence of small scale variability of saturated hydraulic conductivity and porosity, we added a local fluctuation around the average values presented in Table 1, which was generated using the Turning Bands algorithm using two variograms (nugget variogram with sill=0.023; spherical variogram

10 with range=2, and sill=0.047) to generate spatially correlated random fields.

For this typical hillslope a series of simulations were carried out with two different specified boundary conditions. In the first case, the soil is initially fully saturated with or without rainfall events across the hillslope. In this case drainage is occurring over the entire spatial domain of the hillslope, and will reach a steady state after sufficiently

15 long simulation time; this is named the drainage experiment. In the second case, the soil is initially dry and rainfall occurs continuously at a constant rate, and infiltration is the main hydrological process; this is called the infiltration experiment. The boundary conditions used and the mass exchange fluxes required for these studies are described in Fig. 4a. A zero flux boundary condition is assigned to the lower and left boundaries

20 of the slope, as shown in Fig. 4a.

The applied artificial rainfall range is from 0 to 1.0 mm/h in steps of 0.1 mm/h, and 10, 20, 30 and 40 mm/h, which were chosen based on the experience of previous numerical experiments and data interpretation. At rainfall intensities less than 1.0 mm/h, the hillslope becomes almost fully saturated after a 20-month simulation period from 21

25 April 1994 to 31 December 1995; this could be regarded as steady state. It is believed that the most transient solution affecting water dynamics in the Weiherbach catchment could be obtained through these simulations. Based on the analysis of the results from infiltration and drainage experiments, many functional relationships between seepage

EGU

flow and combinations of state variables were tested. The results are presented in Fig. 4b; while the empirical results do display certain multi-valuedness, the general trend is still suggestive of a power law relation. Therefore, as a first step, an empirical closure relation for seepage flow of the following power law form is adopted:

$$e^{os} = \alpha^{os} \left[\frac{S}{|\Psi|} \right]^{\alpha_3^{os}} \tag{22}$$

where S is the degree of saturation estimated over the entire volume of soil (including both the unsaturated and saturated zones), and $|\Psi|$ is the average matric potential head of the soil over the entire unsaturated zone . Both are different from the corresponding point scale values used in Eq. (20) (compare Table 1), and α^{os} and α_3^{os} are parameters that remain to be estimated. The issue of multi-valuedness is important and is left for future research.

Subsequent tests of parameter dependence revealed a relationship of the form $\alpha^{os} = \alpha_1^{os} \overline{K_s}^{\alpha_2^{os}}$, while S is replaced by the ratio of stored water depth in the soil at given time step, $y^u s^u \omega^u + y^s$, to the total soil depth, Z. Accordingly, the closure relation for seepage outflow can be written as:

$$e^{os} = \alpha_1^{os} \overline{K_s}^{\alpha_2^{os}} \left[\frac{y^u s^u \omega^u + y^s}{Z |\Psi|} \right]^{\alpha_3^{os}} \tag{23}$$

The closure relation for seepage flux, or Eq. (23), was developed for the hillslope setting of Fig. 4a, in which seepage flux is only allowed at the right hand side of the slope. Equation (23) must therefore be modified to incorporate the effect of rising water table causing an increase of the seepage face. For this reason, following Sloan and Moore (1984), Eq. (23) is modified to account for water table rise, and this leads to:

$$e^{os} = \omega^o \alpha_1^{os} \overline{K_s}^{\alpha_2^{os}} \left[\frac{y^u s^u \omega^u + y^s}{Z |\Psi|} \right]^{\alpha_3^{os}} \tag{24}$$

3.2.6 Channel flow, and remaining closure relations

For the channel inflow and outflow sections, the following closure relation is suggested based on continuity considerations:

$$\sum_l e_l^{rA} + e_{\text{ext}}^{rA} = \sum_l \frac{m_l^r v_l^r}{\Sigma} - \frac{m^r v^r}{\Sigma} \tag{25}$$

where $\sum_l e_l^{rA}$ are inflow or outflow discharge thorough channel stream network at the inlet or outlet of each REW and e_{ext}^{rA} is outflow discharge at the outlet of the whole catchment system. m_l^r and m^r are channel cross sectional area of the lth neighbouring REW and the REW of interest respectively. v_l^r and v^r are streamflow velocities in channel network at the lth neighbouring REW and the REW of interest respectively. Σ is the projected surface area of the REW of interest onto the horizontal plane.

A small steady groundwater flow is allowed to maintain a minimum water quantity in channel during dry periods, and a zero flux condition is assigned across the REW mantle segment, which is a part of the REW system boundary delimiting the spatial extent of a REW laterally in the subsurface zone. Rainfall or evaporation to and from the c-, o- and r-zones are assumed to be directly proportional to rainfall intensity or potential evaporation multiplied by the area fraction of each zone. All of the closure relations developed above are summarized in Table 2, and compared against the closure relations previously proposed by Reggiani et al. (1999, 2000) on intuitive grounds.

3.3 Constitutive relations for the Weiherbach catchment

3.3.1 Geometric relationship for saturated surface area

It is very important to predict the saturated surface area fraction that responds to saturated zone depth in reasonable way, since the saturated surface area is directly related to the generation of saturation excess overland flow, as well as seepage outflow. Also,

Title Page

Abstract | Introduction

Conclusions | References

Tables | Figures

◀◀ | ▶▶

◀ | ▶

Back | Close

Full Screen / Esc

Printer-friendly Version

Interactive Discussion

EGU

as indicated above, some of the adopted closure relations require the estimate of saturated surface area.

Saturated surface area is the fraction of catchment area caused by the intersection of the water table with the land surface. Hence, it is governed by the dynamics of saturated zone thickness, and by surface topography. Therefore, the relationship between saturated surface area and the depth of saturated zone can be obtained by an understanding of topographic control on saturation area dynamics. In this study, we investigated a possible functional relationship between saturation zone depth and saturated surface area by means of the topographic wetness index of TOPMODEL (Beven and Kirkby, 1979), $\ln\left(a\,[\tan\beta]^{-1}\right)_i$.

Application of TOPMODEL theory to the Weiherbach catchment produced the functional form, shown in Fig. 5, for the geometric relationship between saturated surface area fraction and depth of the saturated zone. This relationship can be expressed as:

$$
\omega^o = \begin{cases} 0 & \text{if } y^s \leq z^r - z^s \\ \dfrac{1}{\beta_1^{\omega^o}+\beta_2^{\omega^o}\exp\left\{-\beta_3^{\omega^o}\left(y^s-Z+|\Psi_b|\right)\right\}} - \dfrac{1}{\beta_1^{\omega^o}+\beta_2^{\omega^o}\exp\left\{-\beta_3^{\omega^o}\left(z^r-z^s-Z+|\Psi_b|\right)\right\}} & \text{if } z^r - z^s < y^s < Z \\ 1 & rmif \ y^s = Z \end{cases}
\tag{26}
$$

where z^r, z^s and Z are average elevation of channel bed from datum, average elevation of the bottom end of the REW above datum, and the average thickness of the subsurface zone respectively, and $\beta_1^{\omega^o}$, $\beta_2^{\omega^o}$ and $\beta_3^{\omega^o}$ are parameters to be estimated. The details of the derivation procedure for the geometric relationship for saturated surface area are shown in Lee et al. (2005b).

3.3.2 REW scale water retention curve: capillary pressure vs. saturation relationship

The REW scale water retention curve represents the soil's matric potential head in the unsaturated zone as a function of the saturation degree also of the unsaturated zone. Similarly, the hydraulic conductivity curve is needed to describe the change of hydraulic

EGU

conductivity with change of saturation degree, at the REW scale, including any effects of the presence of macropores, fractures etc.

The REW scale functional relationship between the soil's matric potential head and saturation degree within the unsaturated zone was derived using the numerical simulation approach. Once again, the distributed model CATFLOW was applied to the Weiherbach catchment. The catchment averages of the soil's matric potential head and saturation degree of the unsaturated zone were estimated through volume averaging of the detailed output from the CATFLOW simulations. The model setting for the CATFLOW simulation is exactly the same as before, except that the spatial domain was the entire catchment. The external boundary condition was specified with observed rainfall taken from 21 April 1994 to 31 December 1995, and not artificial rainfall, since it was thought that a more realistic water retention curve could be derived with this setting.

Based on the analysis of the resulting empirical water retention curves, see Fig. 6a, the following functional relationship between the soil's matric potential head and saturation degree of unsaturated zone was adopted:

$$|\Psi| = \beta_1^{|\Psi|} \{s^u\}^{-\beta_2^{|\Psi|}} \tag{27}$$

where $\beta_1^{|\Psi|}$ is the bubling pressure and $\beta_2^{|\Psi|}$ the pore size distribution index.

3.3.3 Hydraulic conductivity vs. saturation relationship

The procedure adopted for obtaining the hydraulic conductivity curve at the REW scale is identical to the one for the water retention curve. Harmonic averaging was used to estimate the average hydraulic conductivity for a series combination of soil layers, and arithmetic averaging for hydraulic conductivity for a parallel combination of soil layers. In our study, the soil properties are calculated at each node of each hillslope, composed of 21 by 21 nodes, thus the calculation sequence of hydraulic conductivity along nodes as well as on hillslopes may produce different results for the resultant hydraulic conductivity curve at the catchment.

Three alternative methods were devised to estimate catchment scale hydraulic conductivity values. The first method is to use geometric averaging, denoted as $\overline{K_{\text{GEO}}}$; the second method is to use a harmonic average for the series combination of soil layers on each hillslope, as a first step, and then the arithmetic average for parallel combinations, in a second step. The catchment scale hydraulic conductivity obtained from the second method is denoted as $\overline{K_{HA}}$. The third method is the same as the second, except that the steps are reversed, i.e., arithmetic first followed by the harmonic, and the resulting hydraulic conductivity is denoted as $\overline{K_{AH}}$. The results of these calculations are presented in Fig. 6b. On the basis of these it was decided to adopt a power law relationship, of the following form, for the hydraulic conductivity vs. saturation relationship:

$$\overline{K} = \beta_1^{\overline{K}} \{s^u\}^{\beta_2^{\overline{K}}} \tag{28}$$

where $\beta_1^{\overline{K}}$ and $\beta_2^{\overline{K}}$ are parameters that remain to be estimated. Zehe et al. (2006) have proposed an alternative approach for derving the hydraulic conductivity curve based on simulated drainage experiments which just use a single hillslope along with artificial boundary conditions. In contrast to the present approach the hydraulic conductivity is not derived by averaging the values at the model grid nodes but by relating the averaged flux at the lower boundary of the model domain and an expression for the REW-scale recharge velocity in terms of Darcy's law, see Eq. (34) presented below.

3.4 The CREW model

By inserting the derived closure relations into the REW scale mass balance equations, Eqs. (1) to (11), we obtained the basic model equations of the CREW model (Cooperative Community Catchment model based on the Representative Elementary Watershed approach). The 13 balance equations for mass and momentum are reduced to 9 with the aid of a series of assumptions used in Reggiani et al. (2000), which help exclude the momentum balance in the horizontal direction in the two subsurface zones. The

Hydrological modeling with the REW approach

H. Lee et al.

Title Page

Abstract | Introduction

Conclusions | References

Tables | Figures

◀ | ▶

◀ | ▶

Back | Close

Full Screen / Esc

Printer-friendly Version

Interactive Discussion

EGU

resulting equations, including the new closure relations, can now be summarized as follows:

Unsaturated zone mass balance equation

$$\underbrace{\frac{d}{dt}\left(y^u \varepsilon^u \omega^u s^u\right)}_{\text{storage}} = \underbrace{\min\left[i\omega^u,\ \omega^u \overline{K_s}\left(1 + \alpha^{uc}\frac{|\Psi|(1-s^u)\varepsilon^u}{s^u y^u}\right)\right]}_{\text{infiltration}} + \underbrace{\alpha^{us}\omega^u v_z^u}_{\substack{\text{recharge or} \\ \text{capillary rise}}}$$

$$- \underbrace{\min\left[\omega^u\left(e_p + Mk_v\overline{e_p}\right),\ \alpha_{wg}^u \frac{\omega^u \overline{K_s}}{(1-s^u)y^u}\frac{\left(s^u\right)^{2+d}\varepsilon^u|\Psi_b|}{m}\right]}_{\text{evapotranspiration}} \qquad (29)$$

Saturated zone mass balance equation

$$\underbrace{\frac{d}{dt}\left(\varepsilon^s y^s \omega^s\right)}_{\text{storage}} = - \underbrace{\alpha^{us}\omega^u v_z^u}_{\substack{\text{recharge or} \\ \text{capillary rise}}} - \underbrace{\omega^o \alpha_1^{os}\overline{K_s}^{\alpha_2^{os}}\left[\frac{y^u s^u \omega^u + y^s}{Z|\Psi|}\right]^{\alpha_3^{os}}}_{\text{seepage}} - \underbrace{q_s}_{\text{sat. zone−river exchange}} \qquad (30)$$

Concentrated overland flow zone mass balance equation

$$\underbrace{\frac{d}{dt}\left(y^c \omega^c\right)}_{\text{storage}} = \underbrace{\omega^c J}_{\text{rainfall or evaporation}} - \underbrace{\min\left[i\omega^u,\ \omega^u \overline{K_s}\left(1 + \alpha^{uc}\frac{|\Psi|(1-s^u)\varepsilon^u}{s^u y^u}\right)\right]}_{\text{infiltration}}$$

$$- \underbrace{\alpha^{oc}\xi^r y^c v^c}_{\text{flow to saturated overland flow zone}} \qquad (31)$$

EGU

Saturated overland flow zone mass balance equation

$$\underbrace{\frac{d}{dt}\left(y^o\omega^o\right)}_{\text{storage}} = \underbrace{\omega^o\alpha_1^{os}\overline{K_s}^{\alpha_2^{os}}\left[\frac{y^us^u\omega^u + y^s}{Z\,|\Psi|}\right]^{\alpha_3^{os}}}_{\text{seepage}} + \underbrace{\alpha^{oc}\xi^r y^c v^c}_{\text{inflow from conc. overl. flow}}$$

$$+ \underbrace{\omega^o J}_{\text{rainfall or evaporation}} - \underbrace{\alpha^{ro}\xi^r y^o v^o}_{\text{lateral channel inflow}} \qquad (32)$$

Channel zone mass balance equation

$$\underbrace{\frac{d}{dt}\left(m^r\xi^r\right)}_{\text{storage}} = \underbrace{\alpha^{ro}\xi^r y^o v^o}_{\text{lateral channel inflow}} + \underbrace{q_s}_{\text{sat. zone−river exchange}} + \underbrace{\sum_l \frac{m_l^r v_l^r}{\Sigma}}_{\text{inflow}} - \underbrace{\frac{m^r v^r}{\Sigma}}_{\text{outflow}} + \underbrace{\xi^r w^r J}_{\text{rainfall, evaporation on free surface}} \qquad (33)$$

$$v_z^u = \frac{\overline{K}}{y^u}s^u\left[|\Psi| - \frac{1}{2}y^u\right] \qquad (34)$$

$$v^c = \frac{1}{n_m^c}\left[y^c\right]^{2\!/3}\left[\sin\left(\gamma^c\right)\right]^{1\!/2} \qquad (35)$$

$$v^o = \frac{1}{n_m^o}\left[y^o\right]^{2\!/3}\left[\sin\left(\gamma^o\right)\right]^{1\!/2} \qquad (36)$$

$$v^r = \frac{1}{n_m^r}\sqrt{\frac{\left[\overline{R^r}\right]^{1\!/3}}{P^r l^r}\left[m^r l^r\sin\left(\gamma^r\right) \pm \sum_l\left\{\frac{1}{4}y^r\left(m^r + m^l\right)\cos\delta_l\right\} - \frac{1}{2}y^r m^r\right]} \qquad (37)$$

Please note that in doing so, the momentum balance Eq. (8), with respect to the unsaturated zone velocity, v_z^u, has been rewritten as Eq. (34), following the procedure

Title Page

Abstract | Introduction

Conclusions | References

Tables | Figures

|◄ | ►|

◄ | ►

Back | Close

Full Screen / Esc

Printer-friendly Version

Interactive Discussion

EGU

adopted by Reggiani et al. (2000). The momentum balance equations for the c-, o-, and r-zones, i.e., Eqs. (9), (10) and (11), respectively, have been simplified as Eqs. (35), (36) and (37), by adopting the kinematic wave approximation, i.e., by ignoring the inertial term, and by adopting the relationship between Darcy-Weisbach friction factor and

Manning coefficient, $\xi_f^i = 8g \left(n_m^i \right)^2 \left(\overline{R^i} \right)^{-1/3}$, $i=c,o,r$, for the second order friction term, U^i, $i=c,o,r$. The other procedure, which is necessary to convert the momentum balance equation for the channel reach, Eq. (11), into Eq. (37), is presented in Reggiani et al. (2001). Thus, Eqs. (35) and (36) are the REW-scale Manning's equation for the movement over c- and o- zones, respectively, while Eq. (37) is the REW-scale diffusive wave equation for channel flow.

Within the CREW model the balance equations for mass and momentum are solved by the adaptive Runge-Kutta integration method (Press et al., 1992). The current version of CREW model includes a total of 23 parameters: 8 parameters from closure relations (α^{us}, α_1^{os}, α_2^{os}, α_3^{os}, α^{uc}, α_{wg}^{u}, α^{oc}, α^{ro}), 7 parameters from constitutive relations ($\beta_1^{\varpi^o}$, $\beta_2^{\varpi^o}$, $\beta_3^{\varpi^o}$, $\beta_1^{|\Psi|}$, $\beta_2^{|\Psi|}$, $\beta_1^{\overline{K}}$, $\beta_2^{\overline{K}}$), 3 Manning roughness coefficients (n_m^c, n_m^o, n_m^r), porosities of the unsaturated and saturated zone (ε^u, ε^s), canopy density (M), the saturated hydraulic conductivity of the saturated zone (K_s^s), and the ratio of potential rates of transpiration and soil surface evaporation (k_v). All parameters are allowed to be variable across REWs so that the effects of different soil textures, vegetation and geometries across REWs could be taken into account. To run the CREW, the required input information is climate data (rainfall, potential evaporation, and streamflow), and geometric information (length of channel reach at each REW, area of each REW, topographic slopes of the c-, o-, and r-zones, total soil depth, elevation of channel bed from the datum, and the local angle between channel reachs of two neighbouring REWs). Information regarding to soil textures and vegetation can be imported into the modeling procedure by the relevant parameters. Currently, topographic slopes of the c-, o-, and

r-zones are calculated based on the following equation, after Reggiani et al. (1999).

$$\gamma^i = \cos^{-1}\left(\frac{\Sigma^i}{S^i}\right), \quad i = c, o, r \tag{38}$$

where Σ^i is projected area of the i-zone onto the horizontal plane and S^i is the surface area of i-zone. S^i was identified by following the slope in the direction of steepest descent for each grid cell within the digital elevation model and the same S^i value was used for the c-, and o-zones. However, it should be pointed out that topographic slopes of the c-, o-, and r-zones in Eqs. (35) to (37) are effective values defined at the REW scale and they are introduced to account for the balance of forces at the REW scale. Therefore, topographic slopes γ^i should be calculated in a way that they assure balance of momentum in the averaging process, and, at the same time, reflect local geometries of the study area. This may give rise to the problem of parameter estimation by considering γ^i as one of parameters controlling especially the flow routing process.

3.5 Numerical test of the CREW model

Numerical experiments were designed to see how the derived closure relations respond to combinations of climate, soil, vegetation and topography, within the REW modelling framework. Values of the parameters, input data and initial conditions used in the numerical experiments are summarized in Table 3. Two numerical tests were designed. Sensitivity analyses of infiltration and infiltration excess surface runoff generation processes are chosen as the first test, because infiltration excess surface runoff is known as the dominant runoff generation mechanism in Weiherbach catchment. Sensitivity analyses were conducted by changing one variable's value at a time, in each case. The second test was designed to explore streamflow at the outlet as an integrated catchment response combining many interacting processes.

EGU

3.5.1 Infiltration and infiltration excess surface runoff generation

This test is designed to see the effect of antecedent, or initial, moisture content (AMC), rainfall intensity, and different soil types on the infiltration rates, and infiltration excess surface runoff resulting from different rainfall intensities. The effect of AMC on infiltra-
5 tion is modelled by assigning different initial soil moisture contents to the unsaturated zone, while all other inputs are parameters are held fixed. To see the effect of rainfall intensity on infiltration rate and infiltration excess surface runoff, rainfall intensities are varied, while other information such as soil type, AMC etc. are held fixed. Likewise, different soil types are used to see their effects on the infiltration excess runoff process,
10 while other variables held fixed.

For sensitivity analyses of the closure relationship for infiltration, the fixed values chosen are $DI=0.5$, $t_r=2$ days, $t_b=8$ days, $M=0$, $k_v=1$, $n_m^c=0.07\,\mathrm{m}^{-1/3}$ s, $n_m^o=0.035\,\mathrm{m}^{-1/3}$ s, $n_m^r=0.03\,\mathrm{m}^{-1/3}$ s, $q_s=0.00012$ mm/h, $Z=8$ m, $z^r=21$ m, $z^s=20$ m, $\beta_1^{@^o}=0.3$, $\beta_2^{@^o}=0.3$, $\beta_3^{@^o}=0.4$, $\alpha^{uc}=0.1$, $\alpha_{wg}^u=5$, $\alpha^{us}=1$, $\alpha^{oc}=1.5$, $\alpha^{ro}=2.5$, $\alpha_1^{os}=10$,
15 $\alpha_2^{os}=6.2$, $\alpha_3^{os}=2.7$ where DI is the ratio of total annual potential evaporation to total annual precipitation, called the climatic dryness index. In order to fully test the infiltration model, larger unsaturated zone depths are used than in the subsequent test.

Figure 7a shows the effect of AMC of the unsaturated zone on the infiltration rates, for a silty loam, with constant rainfall intensity of 20 mm/h. The results show that as
20 AMC increases, the infiltration rate decreases, the infiltration capacity is higher than rainfall intensity for the smallest AMC used, and that the infiltration rate decreases exponentially after the surface is ponded, which is a well known infiltration behaviour. Figure 7b shows the effect of rainfall intensity, again for a silty loam, when the AMC is zero. The results show that the bigger the rainfall intensity is, the less the time to
25 ponding is, and that regardless of rainfall intensity, the infiltration capacity approaches the same asymptotic value at large time. At lower precipitation intensities, i.e., 1, 5 and 10 mm/h, all precipitation is infiltrated since the infiltration capacity is greater than the rainfall intensity. Figure 7c shows the effect of different soil types, silty loam (solid

EGU

line) and sand (circle), under different rainfall intensities, and zero AMC. Infiltration rate is very high for sandy soils, which is the result of high infiltration capacity. This is confirmed by perusing the infiltration capacity equation, (13), in the light of the soil properties presented in Table 3. The hydraulic conductivity of sand is much higher than that of silty loam, even though bubbling pressure head and porosity are low, which makes the infiltration capacity to be rather high. The infiltration rate for sand at large times decreases smoothly, not exponentially, when rainfall intensity is 40 mm/h. This is different from the results presented in Fig. 7a, and is due to the decrease of the unsaturated area fraction by water table rise, and not due to the occurrence of surface ponding.

Figure 7d shows Hortonian overland flow corresponding to Fig. 7b. Hortonian overland flow accompanies the infiltration process across the concentrated overland flow zone. This is reproduced in Figs. 7b and d. At the end of the storm, i.e., $t > t_r$ Hortonian flow ceases abruptly due to cessation of rainfall. Note here that storm period t_r is defined as the period over which an event lasts without ceasing in the middle; in this study, we used constant values for the storm period along with constant rainfall intensities. On the whole, the water flow dynamics within the concentrated overland flow zone is qualitatively well captured by the adopted closure relations for infiltration capacity and concentrated overland flow, even though the exact magnitude may not be accurate since there has not been any calibration involved, and the question of estimating appropriate parameters remains to be accomplished.

3.5.2 Integrated catchment response measured at the outlet

Figure 8 presents the breakdown of various processes occurring over the catchment in response to a constant intensity event. These include seepage outflow, saturated overland flow and channel flow. The rainfall input is 10 mm/h, and the soil type used was sand. The fixed values are $DI=0.5$, $t_r=2$ days, $t_b=8$ days, $M=1$, $k_v=1$, $n_m^c=0.07 \, \mathrm{m}^{-1/3} \, \mathrm{s}$, $n_m^o=0.035 \, \mathrm{m}^{-1/3} \, \mathrm{s}$, $n_m^r=0.03 \, \mathrm{m}^{-1/3} \, \mathrm{s}$, $q_s=0.00012$ mm/h,

$Z = 8$ m, $z^r = 25$ m, $z^s = 20$ m, $\beta_1^{\omega^o} = 0.3$, $\beta_2^{\omega^o} = 0.3$, $\beta_3^{\omega^o} = 0.4$, $\alpha^{uc} = 1$, $\alpha_{wg}^u = 100$, $\alpha^{us} = 1$, $\alpha^{oc} = 1.5$, $\alpha^{ro} = 2.5$, $\alpha_1^{os} = 2000$, $\alpha_2^{os} = 5.2$, $\alpha_3^{os} = 2.7$. We see in Fig. 8 that the total satu-
rated overland flow is a combined response of both seepage flow and rainfall falling on
saturated areas. There was no Hortonian overland flow from the concentrated overland
5   flow zone in this case, so it can be inferred that the decline of infiltration flux displayed
is not caused due to the reduced soil infiltration capacity or surface ponding, but rather
caused by the increased saturated area fraction. This is confirmed by the surface runoff
caused by rainfall falling on saturated areas. In Fig. 8, the discharge hydrograph at the
catchment outlet is almost the same as saturated overland flow, and does not show
10   any effect of channel storage. This is partly due to the size of catchment used, and the
nature of closure relations used for channel flow. The generalization of these closure
relations to reflect dynamic effects, including diffusion and inertial effects is the subject
of future work.

4   Application of the CREW model to the Weiherbach cachment

15   4.1   Design of simulation tests and set up of the CREW model

The basic idea here is to shed light on the question whether the proposed closure re-
lations and constitutive relations allow reasonable prediction when incorporated within
the CREW model. To achieve this, firstly, the CREW model is set up for the Wei-
herbach catchment and the time series of average soil moisture simulated by CREW is
20   compared against the time series of spatially averaged soil moisture simulated by the
fully distributed model, CATFLOW. The setup of CATFLOW was identical to the model
structure that previously yielded good predictions of soil moisture dynamics, evapo-
transpiration, and runoff in the Weiherbach catchment for a period of 1.5 years (Zehe
et al., 2001). Both models are applied with identical boundary and initial conditions i.e.
25   the observed time series of rainfall and meteorological data.

Title Page

Abstract | Introduction

Conclusions | References

Tables | Figures

◄ | ►

◄ | ►

Back | Close

Full Screen / Esc

Printer-friendly Version

Interactive Discussion

EGU

Secondly, simulation results from the CREW model are compared against (a) observed average soil moisture dynamics and (b) the discharge observed at the outlet of the Weiherbach catchment. This test will show whether the CREW model is able to reproduce realistic soil moisture dynamics derived from 61 TDR stations and, at the
5 same time, the observed rainfall runoff response.

For the Weiherbach catchment, rainfall and streamflow data are available with a temporal resolution of six minutes. As CREW unlike CATFLOW, which uses an advanced SVAT approach based on the Penman-Monteith equation, needs potential evaporation as input for determining actual evaporation, hourly potential evaporation data were
10 generated for the Weiherbach catchment based on the results of Zehe et al. (2001). Slopes of the c-, o-, and r-zones are calculated using Eq. (38) with the use of digital elevation model (DEM) of the catchment. Unsaturated zone depth used was 2 metres for both CREW and CATFLOW. Canopy density (M) was assumed to be equal to 1.0 (unity) for the CREW run, i.e., fully vegetated during the year.

15 ## 4.2 Simulation results

In the first numerical test, the initial saturation of the soil/u-zone was set to 0.5 in both models. One year-long climate time series, measured from 21 April 1994 to 20 April 1995, was used as input to both models. The boundary conditions were chosen in both models such that seepage flux was not allowed. Within CREW we used
20 parameter values directly, without adjustment, obtained from Weiherbach catchment during the upscaling procedure used to develop closure relations and constitutive relations (α^{oc}=1.0, α^{ro}=1.0, $\beta_1^{\circledR^o}$=0.71, $\beta_2^{\circledR^o}$=1.79, $\beta_3^{\circledR^o}$=0.92). However, the average REW scale saturated hydraulic conductivity $\beta_1^{\overline{K}}$ and α_{wg}^u derived with the proposed upscaling did not yield good results. Both parameters were estimated to be 6×10^{-6} m/s
25 and 15.0 respectively in order to reproduce the same s^u times series as predicted by CATFLOW. Figure 9 shows the temporal s^u time series simulated CREW and that the spatially average soil moisture simulated with CATFLOW are in very good agreement.

1703

EGU

EGU

Please note that the results were obtained following minimal calibration.

During the second test, which was aimed at reproducing average observed soil moisture dynamics and rainfall runoff response, again not all the values obtained within the proposed upscaling procedure in Sect. 3 turned out to be useful. In Table 4 we list the parameter values from the proposed upscaling procedures and parameter values obtained through manual calibration using observed rainfall-runoff response, and the associated Nash-Sutcliffe efficiencies.

Especially the REW scale soil hydraulic functions derived with the proposed upscaling were not appropriate, Depending on the averaging procedure (arimethic, geometric, harmonic) we obtained $\beta_1^{\overline{K}}$=3.0×10^{-6}, or 8.0×10^{-7}, or 7.0×10^{-7}, $\beta_2^{\overline{K}}$=1.68, or 1.63, or 1.49. With a manual calibration with hourly data the following values turned out to be acceptable $\beta_1^{|\Psi|}$=0.21, $\beta_2^{|\Psi|}$=0.25, $\beta_1^{\overline{K}}$=8.0×10^{-6}, $\beta_2^{\overline{K}}$=4.51, as they yielded a Nash Sutcliffe efficiency that was larger than 0.8. Interestingly, Zehe et al. (2006) obtained REW scale soil hydraulic functions with almost the same parameter values as the calibrated ones, but a priori, using an advanced upscaling procedure.

Figure 10 compares observed streamflows with those simulated by CREW using parameter values shown in Table 4 above. For presentation purposes, hourly results were aggregated to daily values. Observed hydrograph (Qobs), simulated hydrograph with manually calibrated parameter values (QsimM), and the hydrograph simulated with a priori values obtained from the upscaling procedure (QsimMC) are denoted by crosses, solid line, and dotted line, respectively, as shown in Fig. 10a.

We chose two events for this comparison, denoted as event 1 and event 2 respectively, as shown in Fig. 10a, to compare observed and simulated hydrographs at the event scale. Peak flow for event 1 shown in Fig. 10b is quite well captured by both CREW simulations. During small rainfall events, QsimMC could not capture peak flows well, for example during event 2 shown in Fig. 10c. By investigating the time series of simulated state variables and exchange fluxes of both models, we determined that peak flows predicted by both models during event 1 were mostly produced by infiltration excess overland flow (92 and 94% of streamflow in case of QsimM, and QsimMC

respectively), which supports previous study results on this catchment (Zehe et al., 2005b). However, peak flow produced by QsimM during event 2 was mainly generated by saturation excess overland flow, and contribution of infiltration excess overland flow to peak streamflow was not observed in this case. Runoff contributions of different hydrologic processes for the event 1 and 2 by both simulations are summarized in Figs. 10d, and e. In the case of QsimMC during event 2, due to smaller saturated surface area resulting from three parameters related to Weiherbach catchment geometries ($\beta_1^{\omega^o}$, $\beta_2^{\omega^o}$, and $\beta_3^{\omega^o}$) to estimate saturated surface area as a function of average vertical thickness of saturated zone, there was very small saturation excess overland flow simulated (0.2% of streamflow), and channel flow was mainly due to subsurface flow contributions to the channel. In both model simulations for the event 2, it was found that no infiltration excess overland flow occurred due to the high infiltration capacity when compared to the rainfall intensity. However, in this catchment, the main storm runoff generation mechanism is indeed known as infiltration excess overland flow (Zehe et al., 2005b; Zehe and Blöschl, 2004). This indicates that it might be necessary to revisit the closure relations that are used to predict infiltration excess overland flow, in order to improve the predictive capability of CREW. However, it should be noted that, for the CREW application conducted in this paper, the whole parameter space was not fully searched for the assessment of model performance, which would bring up the problem of appropriate parameter estimation at the catchment scale. In other words, prior to the revision of any closure relations, parameter estimation problem should be sufficiently tackled, unless strong field evidence or previous study indicates inappropriateness of the adopted closure relations.

However, parameter estimation for the CREW is difficult at the present stage due to 1) a lack of any reliable measurement techniques for the estimation of large scale physical properties with high accuracy, 2) insufficient field expemerimental data that is currently available for the parameter estimation at the catchment scale, and 3) unknown range of parameter values at the catchment scale. Therefore, it is extremely important to develop methodologies to estimate parameters at the catchment scale in

EGU

a physically reasonable manner. In this regard, the second numerical test conducted in the paper provides information with regard to the possibility of the usage of the up-scaling procedure as a parameter estimation methodogy for the large scale modeling, which possibly reduces the amount of necessary calibration by estimating parameter values prior to calibration.

We have found good streamflow predictions by manual calibration as shown in Fig. 10 by QsimM, which might prove that CREW is capable of streamflow prediction. However, manual calibration required too much time to get acceptable results due to too many parameters involved in the calibration procedure. If we could estimate at least some of the parameters somehow before relying on the calibration routine, we would definitely reduce the amount of needed calibration. In the second test, streamflow pre-diction by CREW that utilizes parameter estimates from the upscaling procedure was able to capture at least the highest peak streamflow during the simulation period as well as the overall streamflow level during the inter-storm period with a high goodness of fit value, although small streamflow peaks were not captured well. This provides some hope for the utilization of the upscaling procedure as one possible parameter estima-tion procedure, if we remind ourselves that, for streamflow prediction using QsimMC, CREW simulation started from the parameter set for QsimM, and adopted parame-ter estimates from the upscaling procedure without further calibration. This suggests that appropriate upscaling methodologies to estimate large scale physical properties could be an alternative method to solve the problem of parameter estimation at the catchment scale. The development of appropriate upscaling procedure for the param-eter estimation at the catchment scale and the applicability of estimated parameters thorough the procedure for the hydrologic modeling at the catchment scale will be an interesting study topic and is left for the future work.

In the third test, we compared observed soil moisture time series with those modelled by CREW. The streamflow hydrograph is a combined catchment response arising from interactions/feedbacks amongst various fluxes, which together govern the trajectories of the internal state variables. It is therefore essential to compare internal state vari-

EGU

ables, for example, soil moisture content, with observed ones for validation purposes. Weekly measured surface soil moisture data from 61 TDR stations are available in Weiherbach catchment. This data is compared with catchment scale soil moisture content of the unsaturated zone simulated by CREW. Observed soil moisture content is cal-

5 culated by averaging soil moisture data measured at different depth from the surface up to 60 cm. Predictions of s^u by CREW are averaged values over 2 m since 2 m was used as soil depth in the CREW simulations. However, it is still worthwhile to compare observed s^u with simulated ones, considering and acknowledging the uncertainty that possibly results from the spatial heterogeneity and the spatial averaging over the scale

10 of the REW. The comparison between observed s^u and the simulated one is presented in Fig. 11. The observed soil moisture is largely scattered vertically, which reflects temporal and spatial variabilities at the time of measurement. Maximum and minimum observed s^u over a given time step could be used to define the limits of simulated s^u over the same time step. One can see that the simulated s^u curve lies, on the whole,

15 within the range of observed ones. This result may underpin adequate hydrograph fitting through correct description of processes and process interactions within CREW model domain, since their net effect is reflected in the temporal pattern of soil moisture content.

5 Discussion and conclusions

20 In the context of the REW approach of Reggiani et al. (1998, 1999), the development of physically reasonable closure relations for various mass exchange fluxes is a crucial building block, a necessary pre-requisite for the REW approach and associated balance equations to become the basis for a significantly new distributed model blueprint. This paper began with a brief survey of the available methods for the development of

25 closure relations that effectively parameterize the effects of subgrid or sub-REW heterogeneities on the various mass exchange fluxes. Four methods were highlighted: use of detailed field experiments, theoretical/analytical derivations, detailed numerical

[EGU](#)

simulations, and hybrid approaches which may be a combination of any of the above.

In the paper we illustrated the application of some of these methods for the derivation of several closure relations for a representative catchment. For this application we used the Weiherbach catchment in Germany as the example, since (1) there was a wealth of information on catchment physiographic properties and climatic variables, and (2) the catchment was the subject of a detailed field experiment, and detailed information on catchment response, in space and time, including internal state variables and fluxes, were collected as part of this field experiment, (3) a detailed, distributed hydrological model, CATFLOW, has been developed and previously verified using this data. Closure relations for rainfall infiltration, exfiltration, groundwater recharge and capillary rise were derived analytically using various assumptions regarding sub-grid heterogeneity. Closure relations for saturation excess overland flow and concentrated overland flow were derived by a combination of the analytical approach, but assisted by limited numerical models, i.e., by a hybrid approach. Finally, the closure relationship for seepage flow, or subsurface stormflow, was derived by the application of the numerical simulation approach, with the use of the CATFLOW model. The CATFLOW model was also used to derive a new REW-scale pressure-saturation relationship (i.e., water retention curve) and unsaturated hydraulic conductivity versus saturation relationship, which are both required for the parameterization of the momentum balance equation for the unsaturated zone. Finally, a geometric relationship linking saturation area to saturated zone water depth was obtained based on TOPMODEL assumptions.

With the derivation of all of the closure relations and necessary geometric and constitutive relations, the REW scale balance equations are fully determinate, and can be the basis of a spatially distributed (at the REW scale), physically-based model blueprint for the prediction of catchment responses. A complete, and fully determinate numerical model of these coupled set of mass and momentum balance equations, closure relations and geometric relations (i.e., number of equations is equal to the number of unknowns), named CREW, was then used to carry out sensitivity analyses with the view to testing, under realistic conditions, whether the closure relations produced

Hydrological modeling with the REW approach

H. Lee et al.

Title Page

Abstract	Introduction
Conclusions	References
Tables	Figures

◀ | ▶

◀ | ▶

Back | Close

Full Screen / Esc

Printer-friendly Version

Interactive Discussion

estimates of mass fluxes that were physically reasonable when using reasonable parameter values and climatic inputs, while at the same time producing an acceptable overall catchment response. The sensitivity analyses showed that the derived closure relations could indeed describe the dynamics of different hydrological processes in a physically reasonable way under different combinations of climate, soil, vegetation and topography, and also reproduce the expected inherently nonlinear response of the catchment as a whole. In addition to the sensitivity analyses, to assess integrated performance of all developed closure relations in a modelling framework, the predictions of CREW were compared with those of the grid scale physically based distributed model, CATFLOW, by comparing soil moisture dynamics generated by both models. We found that CREW was capable of keeping track of the pattern of soil moisture variation over the period of simulation of CATFLOW, with minimal parameter adjustment, adding credibility to CREW as a consistent catchment scale modelling framework, comparable to CATFLOW. As a final test, we applied CREW to the Weiherbach catchment with parameter values estimated through the upscaling procedure prior to the model run. Prior estimated parameter values, on the whole, brought the model to reasonable predictions in terms of hydrograph fitting, while the parameter values related to the catchment scale water retension curve and hydraulic conductivity-saturation relationship could not improve model performance any further, which is possibly the result of an insufficient search of their whole solution space. Together with this result, further investigation through a comparison of the unsaturated zone saturation values, s^u, simulated by CREW, to the corresponding observed ones, which showed generally good agreement, convinces us that CREW is performing reasonably well at least in terms of predicting catchment streamflow response and describing soil moisture dynamics, both at the catchment scale.

The derivation and successful testing of the various closure relationships for mass exchange fluxes and constitutive relations for momentum balance represent significant step forward in the development of the REW approach. These help to form the foundation of a model blueprint for a new suite of distributed models at the catchment scale,

with the REWs being used as building blocks. For the first time, we now have a complete set of balance equations and associated, physically reasonable, closure relations, leading to a determinate set of balance equations. The numerical implementation of the resulting set of equations into a prototype numerical model, CREW, and its comprehensive testing in an actual catchment are described in a forthcoming paper (Lee et al., 2005a, 2006).

Closure relations derived in this paper thorough the upscaling procedure, with the aid of the scaleway concept as well as the disaggregation-aggregation approach, are preliminary only and are not claimed to be fully satisfactory or final, and should be improved based on improved understanding of hydrological processes from field experiments, and with expert knowledge etc. Closure relations as well as parameter values obtained from Weiherbach catchment can possibly serve to model larger catchments within the same geographical region, which might help reduce the amount of calibration that may be necessary. Closure relations shown in this paper are obtained by explicitly taking into account small scale variabilities into the upscaling procedure, which presumably would provide a better description of the underlying hydrological processes than closure relations derived by conceptual formulation and calibration. We believe that modelling of catchment hydrology based on detailed understanding of the study area, for example by deriving closure relations for the Weiherbach catchment by incorporating the textures, structures and material properties that are present into account, would definitely assist hydrologists, in the long term, towards resolving the PUB problem.

Appendix A

Derivation of a closure relation for bare soil evaporation and transpiration by root uptake (e_{wg}^u)

One dimensional concentration dependent diffusion equation describing soil moisture movement in the unsaturated zone (Philip, 1960) has the following form, when it includes a soil moisture extraction term by root uptake as a sink (Eagleson, 1978a):

$$\frac{\partial \theta}{\partial t} = \frac{\partial}{\partial t}\left[D(\theta)\frac{\partial \theta}{\partial z}\right] - \frac{\partial K(\theta)}{\partial z} - g_r(z,\theta) \tag{A1}$$

where θ is the effective volumetric moisture content, t is time, $K(\theta)$ is the effective hydraulic conductivity, $D(\theta)$ is the diffusivity, $g_r(z,\theta)$ root extraction function, and z is vertical coordinate. In analogy with the infiltration capacity equation of Philip (1960), Eagleson (1978b) derived an exfiltration capacity equation as:

$$f_e^* \approx \frac{1}{2}S_e t^{-\frac{1}{2}} - Me_v \tag{A2}$$

where f_e^* is exfiltration capacity for bare soil evaporation, M is canopy density, and e_v is transpiration rate. In Eq. (A2), S_e is an exfiltration sorptivity defined by:

$$S_e = 2(\theta_0 - \theta_1)\left[\frac{D_e}{\pi}\right]^{\frac{1}{2}} \tag{A3}$$

where θ_0 is initial effective volumetric moisture content, θ_1 is effective volumetric moisture content at the soil surface, and D_e is a desorption diffusivity defined by:

$$D_e = \frac{K_s|\Psi_b|s_0^d \phi_e}{m\varepsilon} \tag{A4}$$

where K_s is the saturated hydraulic conductivity, $|\Psi_b|$ is bubbling pressure head, s_0 is initial degree of saturation at the soils surface, where this value is fixed by "zeroth-order" approximation at a space-time average soil moisture (Eagleson, 1978a), d is

Title Page

Abstract | Introduction

Conclusions | References

Tables | Figures

◄◄ | ►►

◄ | ►

Back | Close

Full Screen / Esc

Printer-friendly Version

Interactive Discussion

EGU

a diffusivity index, m is the pore size distribution index, ε is soil porosity, and ϕ_e is a dimensionless exfiltration diffusivity defined as:

$$\phi_e = 1.85 s_0^{-1.85-d} \int_0^{s_0} s^d (s_0 - s)^{0.85} \, ds \tag{A5}$$

Now let us define combined evapotranspiration capacity, f_{ET}^*, by both bare soil evaporation and transpiration by root uptake, as follows:

$$f_{ET}^* = f_e^* + Me_v \tag{A6}$$

If Eq. (A4) is substituted into Eq. (A3), with the condition θ_1 is equal to zero for exfiltration, then we have:

$$S_e = S_{er} K_s^{\frac{1}{2}} \tag{A7}$$

$$S_{er} = 2s_0 \left[\frac{|\Psi_b| \varepsilon s_0^d \phi_e}{m\pi} \right]^{\frac{1}{2}} \tag{A8}$$

where S_{er} is an exfiltration sorptivity coefficient, assumed to be constant for a soil type, and only K_s is spatially variable in Eq. (A7). This assumption could be justified by the same reason as offered by Bresler and Dagan (1983), K_s has the greatest impact on the exfiltration process. As before, K_s is also assumed to follow a lognormal distribution. Combining Eqs. (A2), (A6) and (A7), we then obtain:

$$f_{ET}^* = \frac{1}{2} S_{er} K_s^{\frac{1}{2}} t^{-\frac{1}{2}} \tag{A9}$$

Taking the areal average of Eq. (A9), we obtain an equation for the areal average exfiltration capacity:

$$\overline{f_{ET}^*} = \frac{1}{2} S_{er} \overline{K_s^{\frac{1}{2}}} t^{-\frac{1}{2}} \tag{A10}$$

Title Page

Abstract | Introduction

Conclusions | References

Tables | Figures

◄◄ | ►►

◄ | ►

Back | Close

Full Screen / Esc

Printer-friendly Version

Interactive Discussion

EGU

The average exfiltration capacity equation, Eq. (A10), depends on time, which makes its applicability in for continuous modeling, so we need to convert it into time independent form. For this reason, it is assumed that the exfiltration capacity is a function of the volume of cumulative exfiltration only, in analogy with the Time Condensation Approximation (Sherman, 1943) used for infiltration. Then, the cumulative volume of exfiltration can be obtained by integration of Eq. (A9) as:

$$F_{ET} = S_{er} K_s^{\frac{1}{2}} t^{\frac{1}{2}} \tag{A11}$$

which means that the areal average of the cumulative volume of exfiltration will be:

$$\overline{F_{ET}} = S_{er} \overline{K_s^{\frac{1}{2}}} t^{\frac{1}{2}} \tag{A12}$$

If we eliminate $t^{\frac{1}{2}}$ between Eqs. (A12) and (A10) we obtain:

$$\overline{f_{ET}^*} = \frac{1}{2} \frac{S_{er}^2 \left[\overline{K_s^{1/2}}\right]^2}{\overline{F_{ET}}} \tag{A13}$$

Since K_s is assumed to follow a lognormal distribution, following Rogers (1992), $\left[\overline{K_s^{1/2}}\right]^2$ can be replaced by following relationship

$$\left[\overline{K_s^{1/2}}\right]^2 = \overline{K_s} \exp\left(-\frac{\sigma_n^2}{4}\right) \tag{A14}$$

1713

where σ_n^2 is the variance of logarithm of K_s. If we now combine Eqs. (A8) and (A14), and substitute in Eq. (A13), we will finally obtain:

$$\overline{f_{ET}^*} = \alpha \frac{\overline{K_s}}{\overline{F_{ET}}} \frac{s_0^{2+d} \varepsilon |\Psi_b|}{m} \tag{A15}$$

where $\alpha = \frac{2\phi_e}{\pi} \exp\left(-\frac{\sigma_n^2}{4}\right)$ is an estimatable parameter that is related to the variability of saturated hydraulic conductivity, and the dimensionless exfiltration diffusivity ϕ_e. To use Eq. (A15) within the REW approach, it is assumed that the spatial average of the cumulative volume of exfiltration is proportional to the pore fraction that is not filled with water, i.e., $\overline{F_{ET}} \approx (1-s^u)\, y^u$, where the initial degree of saturation at the soil surface is replaced by the saturation degree of the entire unsaturated zone. Consequently, we obtain the following exfiltration capacity equation:

$$\overline{f_{ET}^*} = \alpha \frac{\overline{K_s}}{(1-s^u)\, y^u} \frac{(s^u)^{2+d} \varepsilon |\Psi_b|}{m} \tag{A16}$$

Therefore, the final closure relation, for the combination of bare soil evaporation and transpiration by root water uptake, will be specified as:

$$e_{wg}^u = \min\left[(e_p + M\overline{e_v})\, \omega^u, \quad \overline{f_{ET}^*}\, \omega^u \right] \tag{A17}$$

where $\overline{e_v}$ is spatially averaged transpiration rate at each time step. Since this may not be available in most catchments, it is assumed that $\overline{e_v}$ is constant and equal to long-term time average potential rate of transpiration $\overline{e_{pv}}$. By using the ratio $k_v = \frac{\overline{e_{pv}}}{\overline{e_p}}$, where $\overline{e_p}$ is long-term time average rate of potential (soil-surface) evaporation, the probable maximum exfiltration rate, $\overline{f_{ET}}\Big|_{max}$, at each time step, will be expressed by:

$$\overline{f_{ET}}\Big|_{max} = e_p + M k_v \overline{e_p} \tag{A18}$$

EGU

and the corresponding closure relation is written as:

$$e_{wg}^u = \min\left[\left(e_p + Mk_v\overline{e_p}\right)\varpi^u, \quad \overline{f_{ET}^*}\varpi^u\right]$$ (A19)

Hydrological modeling with the REW approach

H. Lee et al.

Full Screen / Esc

Printer-friendly Version

Interactive Discussion

EGU

Appendix B

Nomenclature

Latin symbols

A	mantle surface with horizontal normal delimiting the REW externally	
A	linearisation coefficient for the mass exchange terms	$[TL^{-1}]$
B	linearisation coefficient for the mass exchange terms	$[ML^{-3}]$
c	pore disconnectedness index	
d	diffusivity index	
$\overline{d}$	depth of pore contained in a surface soil layer	$[L]$
D	diffusivity	$[L^2T^{-1}]$
$\overline{D}$	depth of a surface soil layer	$[L]$
D_e	desorption diffusivity	$[L^2T^{-1}]$
DI	dryness index, or the ratio of annual potential evaporation to annual precipitation	
e	water mass exchange per unit surface area divided by water mass density	$[LT^{-1}]$
e_p	potential evaporation rate from a bare soil surface	$[LT^{-1}]$
$\overline{e_p}$	long term time average rate of potential (soil surface) evaporation	$[LT^{-1}]$
$\overline{e_{pv}}$	long-term time average potential rate of transpiration	$[LT^{-1}]$
e_v	transpiration rate at the point scale	$[LT^{-1}]$
$\overline{e_v}$	spatially averaged transpiration rate	$[LT^{-1}]$

5

Title Page

Abstract | Introduction

Conclusions | References

Tables | Figures

◄◄ | ►►

◄ | ►

Back | Close

Full Screen / Esc

Printer-friendly Version

Interactive Discussion

EGU

f	a parameter controlling the exponential decline of transmissivity with depth	$[L^{-1}]$
$\overline{f^*}$	spatially averaged infiltration capacity	$[LT^{-1}]$
f_e^*	exfiltration capacity for bare soil evaporation	$[LT^{-1}]$
f_{ET}^*	evapotranspiration capacity by exfiltration of water from subsurface	$[LT^{-1}]$
$\overline{f_{ET}^*}$	spatially averaged exfiltration capacity on bare soil evaporation and transpiration by root uptake	$[LT^{-1}]$
f_M	macro-porosity factor	
$\overline{F}$	spatially averaged cumulative volume of infiltration	$[L]$
F_{ET}	cumulative volume of evapotranspiration by exfiltration	$[L]$
$\overline{F_{ET}}$	spatially averaged cumulative volume of evapotranspiration by exfiltration	$[L]$
g	gravitational acceleration	$[LT^{-2}]$
g_r	root extraction function	
h_f	free water content	$[L]$
i	rainfall intensity	$[LT^{-1}]$
J	rate of rainfall input or evaporation	$[LT^{-1}]$
k_v	ratio of potential rates of transpiration and soil surface evaporation	
K	hydraulic conductivity at the point scale	$[LT^{-1}]$
$\overline{K}$	hydraulic conductivity at the catchment scale	$[LT^{-1}]$
K^B	bulk hydraulic conductivity	$[LT^{-1}]$
K_s	saturated hydraulic conductivity at the point scale	$[LT^{-1}]$
$\overline{K_s}$	mean saturated hydraulic conductivity	$[LT^{-1}]$
l_i	wetness index at grid point i, or $\ln\left(a\,[\tan\beta]^{-1}\right)_i$	

Hydrological modeling with the REW approach

H. Lee et al.

Title Page

Abstract	Introduction
Conclusions	References
Tables	Figures

◄◄ ►►

◄ ►

Back Close

Full Screen / Esc

Printer-friendly Version

Interactive Discussion

EGU

l^r	the length of a channel reach	[L]
L	the length of a slope unit	[L]
M	vegetated fraction of land surface, or canopy density	
m	pore size distribution index	
$\overline{m}$	constant used in kinematic wave equation (Ichikawa and Shiiba, 2002)	
m^r	average channel cross sectional area	[L^2]
N	constant used in kinematic wave equation (Ichikawa and Shiiba, 2002)	
n_m	Manning roughness coefficient	$\left[TL^{-1/3}\right]$
n	shape parameter	
p	pressure	[FL^{-2}]
P	the wetted perimeter	[L]
q	hillslope discharge per unit width	[L^2T^{-1}]
q_s	steady flow from saturated zone to channel reach	[LT^{-1}]
R	first order friction term	[FTL^{-3}]
$\overline{R}$	the hydraulic radius	[L]
s	the saturation function of unsaturated zone at the point scale	
s^u	the saturation function of unsaturated zone at the catchment scale	
s_0	initial degree of saturation in surface boundary layer	
$\overline{s_0}$	threshold value of saturation function for macropore flow	
S	saturation degree of the entire volume of soil media	
$\overline{S}$	storage volume of a slope unit	[L^3]
S_e	exfiltration sorptivity	[$LT^{-0.5}$]

Hydrological modeling with the REW approach

H. Lee et al.

Full Screen / Esc

Printer-friendly Version

Interactive Discussion

EGU

S_{er}	exfiltration sorptivity coefficient	$[L^{0.5}]$
t	time	$[T]$
t_r	storm period	$[T]$
t_b	inter-storm period	$[T]$
t_a	climatic period	$[T]$
U	second order friction term	$[FT^2 L^{-4}]$
$\overline{U}$	the upslope contributing area of a slope unit	$[L^2]$
v	velocity of bulk phases	$[LT^{-1}]$
$\overline{w}$	average width of a slope unit	$[L]$
w^r	top width of the channel	$[L]$
y	average vertical thickness	$[L]$
Z	average thickness of the subsurface zone	$[L]$
z	vertical coordinate	$[L]$
$\bar{z}$	average water table depth from the ground surface	$[L]$
z^r	average elevation of channel bed from datum	$[L]$
z^s	average elevation of the bottom end of the REW from datum	$[L]$

Hydrological modeling with the REW approach

H. Lee et al.

Title Page

Abstract	Introduction
Conclusions	References
Tables	Figures

|◄ | ►|

◄ | ►

Back | Close

Full Screen / Esc

Printer-friendly Version

Interactive Discussion

EGU

Greek symbols

α a parameter

$\bar{\alpha}$ air entry value $[L^{-1}]$

β a parameter

δ_l the local angle between the reach of the REW l and the reach of the REW under consideration

γ_c field capacity

γ_e effective porosity

γ^i slope angle of the i-subregion flow plane with respect to the horizontal plane

η the slope gradient of a slope unit

ε soil porosity

$\bar{\lambda}$ expectation of wetness index l_i

θ effective volumetric moisture content

θ_0 initial effective volumetric moisture content

θ_1 effective volumetric moisture content at surface of medium

θ_i initial soil moisture content

θ_r residual water content

θ_s saturated soil moisture content

ρ water mass density $[ML^{-3}]$

σ_n^2 the variance of logarithm of saturated hydraulic conductivity

Σ projection of the total REW surface area onto the horizontal plane $[L^2]$

ξ_f Darcy-Weisbach friction factor

EGU

ξ^r	the length of the main channel reach per unit surface area projection	$[L^{-1}]$
$\|\psi\|$	soil matric potential head of unsaturated zone at the point scale	$[L]$
$\|\Psi\|$	soil matric potential head of unsaturated zone at the catchment scale	$[L]$
$\|\Psi_b\|$	bubbling pressure head	$[L]$
$\|\Psi_f\|$	soil matric potential head at the wetting front	$[L]$
ϕ	the gravitational potential	
ϕ_e	dimensionless exfiltration diffusivity	
ω	time averaged surface area fraction	

Subscripts and superscripts

bot	superscript for the region delimiting the domain of interest at the bottom
l	subscript indicating the various REWs within the watershed
top	superscript for the atmosphere, delimiting the domain of interest at the top
u,s,c,o,r	superscripts indicating subregions within a REW
w, g	designate the water and the gaseous phase respectively
$^{jA}_{ext}$	exchange from the j-subregion across the external watershed boundary
$^{jA}_{l}$	exchange from the j-subregion across the lth mantle segment

References

Attinger, S.: Generalized coarse graining procedures for flow in porous media, Comp. Geosci., 7, 253–273, 2003.

Beven, K. J.: Towards an alternative blueprint for a physically based digitally simulated hydrologic response modelling system, Hydrol. Processes, 16, 189–206, 2002.

Beven, K. J. and Kirkby, M. J.: A physically-based variable contributing area model of basin hydrology, Hydrol. Sci. Bull., 24(1), 43–69, 1979.

Blöschl, G. and Zehe, E.: On hydrological predictability, Hydrol. Processes, 19(9), 3923–3929, 2005.

Bras, R. L.: Hydrology: An Introduction to Hydrologic Science, Reading, Mass., USA, Addison-Wesley-Longman, 1990.

Bresler, E. and Dagan, G.: Unsaturated flow in spatially variable fields. 2. Application of water flow models to various fields, Water Resour. Res., 19(2), 421–428, 1983.

Chow, V. T., Maidment, D. R., and Mays, L. W.: Applied Hydrology, McGraw-Hill, Inc, 1988.

Dagan, G.: Flow and Transport in Porous Formations, Springer-Verlag, New York, 1989.

Duffy, C. J.: A two-state integral-balance model for soil moisture and groundwater dynamics in complex terrain, Water Resour. Res., 32(8), 2421–2434, 1996.

Eagleson, P. S.: Climate, soil, and vegetation, 1. Introduction to water balance dynamics, Water Resour. Res., 14(5), 705–712, 1978a.

Eagleson, P. S.: Climate, soil, and vegetation, 3. A simplified model of soil moisture movement in the liquid phase, Water Resour. Res., 14(5), 722–730, 1978b.

Eagleson, P. S.: Climate, soil, and vegetation, 4. The expected value of annual evapotranspiration, Water Resour. Res., 14(5), 731–739, 1978c.

Ichikawa, Y. and Shiiba, M.: Lumping of kinematic wave equation considering field capacity, 3rd Int. Conf. Water Resour. Environ. Res., 2002.

Kees, C. E., Band, L. E., and Farthing, M. W.: Effects of Dynamic Forcing on Hillslope Water Balance Models, Technical Report CRSC-TR04-12, Center for Research in Scientific Computation, Department of Mathematics, North Carolina State University, 2004.

Kees, C. E., Farthing, M. W., Band, L. E., and Miller, C. T.: Choices of scale and process complexity in hillslope models, Eos Trans. AGU, 83(47), Fall Meet. Suppl., Abstract H62B-0838, 2002.

Lee, H., Sivapalan, M., and Zehe, E.: Representative Elementary Watershed (REW) approach,

a new blueprint for distributed hydrologic modelling at the catchment scale, in: Predictions in ungauged basins: international perspectives on state-of-the-art and pathways forward, edited by: Franks, S. W., Sivapalan, M., Takeuchi, K., and Tachikawa, Y., IAHS Press, Wallingford, Oxon, UK, 2005a.

5 Lee, H., Sivapalan, M., and Zehe, E.: Representative Elementary Watershed (REW) approach, a new blueprint for distributed hydrologic modelling at the catchment scale: the development of closure relations, in: Predicting ungauged streamflow in the mackenzie river basin: today's techniques & tomorrow's solutions, edited by: Spence, C., Pomeroy, J. W., and Pietroniro, A., Canadian Water Resour. Assoc. (CWRA), Ottawa, Canada, 165–218, 2005b.

10 Lee, H., Sivapalan, M., and Zehe, E.: Representative Elementary Watershed (REW) approach, a new blueprint for distributed hydrologic modelling at the catchment scale: Numerical implementation, in: Physically based models of river runoff and their application to ungauged basins, Proceedings, NATO Advanced Research Workshop, edited by: O'Connell, P. E. and Kuchment, L., Newcastle-upon-Tyne, UK, in press, 2006.

15 Lunati, I., Attinger, S., and Kinzelbach, W.: Macrodispersivity for transport in arbitrary nonuniform flow fields: Asymptotic and pre-asymptotic results, Water Resour. Res., 38(10), 1187, doi:10.1029/2001WR001203, 2002.

Maurer, T.: Physikalisch begrundete, zeitkontinuierliche Modellierung des Wassertransports in kleinen landlichen Einzugsgebieten. Universitat Karlsruhe, Mitteilungen Inst. F. Hydrologie u.
20 Wasserwirtschaft, H. 61, Universitat Karlsruhe, 1997.

Mualem, Y.: A new model for predicting the hydraulic conductivity of unsaturated porous media, Water Resour. Res., 12, 513–522, 1976.

Philip, J. R.: General method of exact solution of the concentration-dependent diffusion equation, Aust. J. Phys., 13(1), 1–12, 1960.

25 Press, W. H., Teukolsky, S. A., Vetterling, W. T., and Flannery, B. P.: Numerical Recipes in FORTRAN, Cambridge University Press, 1992.

Reggiani, P. and Schellekens, J.: Modelling of hydrological responses: the representative elementary watershed approach as an alternative blueprint for watershed modelling, Hydrol. Processes, 17, 3785–3789, 2003.

30 Reggiani, P., Sivapalan, M., and Hassanizadeh, S. M.: A unifying framework for watershed thermodynamics: balance equations for mass, momentum, energy and entropy and the second law of thermodynamics, Adv. Water Resour., 22(4), 367–398, 1998.

Reggiani, P., Hassanizadeh, S. M., Sivapalan, M., and Gray, W. G.: A unifying framework for

Hydrological modeling with the REW approach

H. Lee et al.

EGU

watershed thermodynamics: constitutive relationships, Adv. Water Resour., 23(1), 15–39, 1999.

Reggiani, P., Sivapalan, M., and Hassanizadeh, S. M.: Conservation equations governing hillslope responses: exploring the physical basis of water balance, Water Resour. Res., 36(7), 1845–1863, 2000.

Reggiani, P., Sivapalan, M., Hassanizadeh, S. M., and Gray, W. G.: Coupled equations for mass and momentum balance in a stream network: theoretical derivation and computational experiments, Proc. R. Soc. Lond., 457, 157–189, 2001.

Robinson, J. S. and Sivapalan, M.: Catchment-scale runoff generation model by aggregation and similarity analyses, Hydrol. Processes, 9, 555–574, 1995.

Robock, A., Vinnikov, K. Y., Srinivasan, G., Entin, J. K., Hollinger, S. E., Speranskaya, N. A., Liu, S., and Namkhai, A.: The Global Soil Moisture Data Bank, Bull. Amer. Meteor. Soc., 81, 1281–1299, 2000.

Rogers, A. D.: The development of a simple infiltration capacity equation for spatially variable soils. B.E (Honours) thesis, Department of Civil and Environmental Engineering, The University of Western Australia, 1992.

Schäfer, D.: Bodenhydraulische Eigenschaften eines Kleineinzugsgebiets – Vergleich und Bewertung unterschiedlicher Verfahren, PhD dissertation, Institute of Hydromechanics, University of Karlsruhe, Germany, 1999.

Schulz, K., Seppelt, R., Zehe, E., Vogel, H. J., and Attinger, S.: Importance of spatial structures in advancin hydrological sciences, Water Resour. Res., 42(3), W03S03, doi:10.1029/2005WR004301, 2006.

Sherman, L. K.: Comparison of F-curves derived by the methods Sharp and Holtan and of Sherman and Mayer, Trans. Am. Geophys. Un., 24, 465–467, 1943.

Sivapalan, M.: Linking hydrologic parameterizations across a range of spatial scales: hillslope to catchment to region, IAHS Publication Number 212, Proc. Yokohama Symposium, 115–123, 1993.

Sivapalan, M., Takeuchi, K., Franks, S. W., Gupta, V. K., Karambiri, H., Lakshmi, V., Liang, X., McDonnell, J. J., Mendiondo, E. M., O'Connel, P. E., Oki, T., Pomeroy, J. W., Schertzer, D., Uhlenbrook, S., and Zehe, E.: IAHS decade on Predictions of Ungauged Basins (PUB): Shaping an exciting future for the hydrological sciences, Hydrol. Sci. J., 48(6), 857–879, 2003.

Sloan, P. G. and Moore, I. D.: Modeling subsurface stormflow on steeply sloping forested wa-

Title Page

Abstract | Introduction

Conclusions | References

Tables | Figures

◄ | ►►

◄ | ►

Back | Close

Full Screen / Esc

Printer-friendly Version

Interactive Discussion

EGU

tersheds, Water Resour. Res., 20(12), 1815–1822, 1984.

van Genuchten, M. T.: A closed-form equation for predicting the hydraulic conductivity of unsaturated soils, Soil Sci. Soc. Amer. J., 44, 892–898, 1980.

Viney, N. R. and Sivapalan, M.: A framework for scaling of hydrologic conceptualisations based on a disaggregation-aggregation approach, Hydrol. Processes, 18, 1395–1408, 2004.

Vogel, H. J. and Roth, K.: Moving through scales of flow and transport in soil, J. Hydrol., 272, 95–106, 2003.

Western, A. W. and Grayson, R. B.: The Tarrawarra data set: soil moisture patterns, soil characteristics and hydrological flux measurements, Water Resour. Res., 34(10), 2765–2768, 1998.

Zehe, E., Maurer, T., Ihringer, J., and Plate, E.: Modeling water flow and mass transport in a Loess catchment, Phys. Chem. Earth (B), 26, 7–8, 487–507, 2001.

Zehe, E. and Blöschl, G.: Predictability of hydrologic response at the plot and catchment scales – the role of initial conditions, Water Resour. Res., 40(10), W10202, doi:10.1029/2003WR002869, 2004.

Zehe, E., Lee, H., and Sivapalan, M.: Derivation of closure relations and commensurate state variables for mesoscale hydrological models using dynamical upscaling, in: Predictions in ungauged basins: international perspectives on state-of-the-art and pathways forward, edited by: Franks, S. W., Sivapalan, M., Takeuchi, K., and Tachikawa, Y., IAHS Press, Wallingford, Oxon, UK, 2005a.

Zehe, E., Becker, R., Bardossy, A., and Plate, E.: Uncertainty of simulated catchment runoff response in the presence of threshold processes: Role of initial soil moisture and precipitation, J. Hydrol., 315, 183–202, 2005b.

Zehe, E., Lee, H., and Sivapalan, M.: Dynamical process upscaling for deriving catchment scale state variables and constitutive relations for meso-scale process models, Hydrol. Earth Syst. Sci. Discuss., 3, 1629–1665, 2006.

Title Page

Abstract | Introduction

Conclusions | References

Tables | Figures

◄ | ►

◄ | ►

Back | Close

Full Screen / Esc

Printer-friendly Version

Interactive Discussion

EGU

Table 1. Laboratory measurements of average hydraulic properties for typical Weiherbach soils. Definition of parameters after van Genuchten (1980) and Mualem (1976). Saturated hydraulic conductivity K_s, porosity ε, residual water content θ_r, air entry value $\bar{\alpha}$, shape parameter n.

	K_s [m s^{-1}]	ε [m^{3}m^{-3}]	θ_r [m^{3}m^{-3}]	$\bar{\alpha}$ [m^{-1}]	n [–]
Calcareous regosol	2.1×10^{-6}	0.44	0.06	0.40	2.06
Colluvisol	6.1×10^{-6}	0.40	0.04	1.90	1.25

EGU

Table 2. Closure relations for exchanging mass flux.

Flux term	Closure relations (Reggiani et al., 1999, 2000)	Closure relations (this paper)
Infiltration (e^{uc})	$\min\left[i\omega^u, \ \frac{\overline{K_s}\omega^u}{s^u y^u}\left(-\lvert\Psi_b\rvert\left(s^u\right)^{-1}/\mu + \frac{1}{2}y^u\right)\right]$	$\min\left[i\omega^u, \ \omega^u\overline{K_s}\left(1+\alpha^{uc}\frac{\lvert\Psi\rvert(1-s^u)\varepsilon^u}{s^u y^u}\right)\right]$
Evapotranspiration (e^u_{wg})	$\omega^u s^u e_p$	$\min\left[\omega^u\left(e_p+Mk_v\overline{e_p}\right), \ \alpha^u_{wg}\frac{\omega^u\overline{K_s}}{(1-s^u)y^u}\frac{\left(s^u\right)^{2+d}\varepsilon^u\lvert\Psi_b\rvert}{m}\right]$
Recharge or Capillary rise (e^{us})	$\varepsilon\omega^u v^u_z$	$\alpha^{us}\omega^u v^u_z$
Saturated overland flow (e^{ro})	$\frac{B^{or}\Lambda^{or}y^o v^o}{\rho}$	$\alpha^{ro}\xi^r y^o v^o$
Concentrated overland flow (e^{oc})	$\frac{B^{co}\Lambda^{co}(y^o+y^c)(v^o+v^c)}{4\rho}$	$\alpha^{oc}\xi^r y^c v^c$
Seepage flow (e^{os})	$\frac{\overline{K_s}\omega^o}{\cos(\gamma^o)\Lambda_s}\frac{1}{2}\left[y^s-z^r+z^s\right]$	$\omega^o\alpha^{os}_1\overline{K_s}^{\alpha^{os}_2}\left[\frac{y^u s^u\omega^u+y^s}{Z\lvert\Psi\rvert}\right]^{\alpha^{os}_3}$
Inflow and outflow at channel reach ($\sum_l e^{rA}_l+e^{rA}_{ext}$)	$\pm\sum_l\frac{B^{rA}_l A^{rA}_l\left(v^r+v^r\lvert_l\right)}{2\rho}+e^{rA}_{ext}$	$\sum_l\frac{m^r_l v^r_l}{\Sigma}-\frac{m^r v^r}{\Sigma}$
Rainfall or evaporation at C-zone (e^{ctop})	$\omega^c J$	$\omega^c J$
Rainfall or evaporation at O-zone (e^{otop})	$\omega^o J$	$\omega^o J$
Rainfall or evaporation at R-zone (e^{rtop})	$\omega^r J$	$\omega^r J$
Ground flow to channel (e^{rs})	$A^{sr}\left[\frac{p^r-p^s}{\rho}+\phi^r-\phi^s\right]$	q_s
Mass exchange across mantle segment at U-zone ($\sum_l e^{uA}_l+e^{uA}_{ext}$)	$\sum_l B^{uA}_l\frac{1}{2\rho}[\pm A^{uA}_{l,x}(v^u_x+v^u_x\lvert_l)$ $+\pm A^{uA}_{l,y}(v^u_y+v^u_y\lvert_l)]+e^{uA}_{ext}$	Zero flux boundary condition
Mass exchange across mantle segment at S-zone ($\sum_l e^{sA}_l+e^{sA}_{ext}$)	$\sum_l B^{sA}_l\frac{1}{2\rho}[\pm A^{sA}_{l,x}(v^s_x+v^s_x\lvert_l)$ $+\pm A^{sA}_{l,y}(v^s_y+v^s_y\lvert_l)]+e^{sA}_{ext}$	Zero flux boundary condition

Table 3. Values of parameters, input data and initial conditions used in the sensitivity analysis.

Group	Description		Value	Reference
Soil	K_s: saturated hydraulic conductivity [m/s]	Silty loam	3.4×10^{-6}	Bras (1990)
		Sandy loam	3.4×10^{-5}	
		Sand	8.6×10^{-5}	
	$|\Psi_b|$: bubbling pressure head [m]	Silty loam	0.45	
		Sandy loam	0.25	
		Sand	0.15	
	ε: porosity [m^3/m^3]	Silty loam	0.35	
		Sandy loam	0.25	
		Sand	0.20	
	m: pore size distribution index	Silty loam	1.2	
		Sandy loam	3.3	
		Sand	5.4	
	c: pore disconnectedness index	Silty loam	4.7	
		Sandy loam	3.6	
		Sand	3.4	
	$s^u(0)$: initial soil moisture content in U-zone		0.0/0.1/0.2/0.3/0.4/0.5	
Climate	i: precipitation intensity [mm/h]		1/5/10/20/30/40	
	DI: climatic dryness index		0.5/1.0/2.0	
	t_r: storm period [day]		2	
	t_b: inter-storm period [day]		8	
	$t_a(=t_r+t_b)$: Climatic period [day]		10	
Vegetation	M: canopy density		0.0/0.5/1.0	
	k_v: ratio of potential rates of transpiration and soil surface evaporation		1	
Hydraulic	n_m^c: Manning roughness coefficient in the c-zone [m$^{-1/3}$ s]		0.07	Chow et al. (1988)

Table 3. Continued.

Group	Description	Value	Reference
	n_m^o: Manning roughness coefficient in the o-zone [$m^{-1/3}$ s]	0.035	
	n_m^r: Manning roughness coefficient in the r-zone [$m^{-1/3}$ s]	0.03	
	q_s: assumed steady flow from saturated zone to channel reach [mm/h]	0.00012	
Geographic	Z: average thickness of the subsurface zone [m]	8	
	z^r: average elevation of channel bed from datum [m]	21/25	
	z^s: average elevation of the bottom end of REW from datum [m]	20	
	$y^s(0)$: initial average thickness of saturated zone [m]	$z^r - z^s$	
	$\beta_1^{@^o}$: a geometric parameter in the saturated surface area function	0.3/0.59942	
	$\beta_2^{@^o}$: a geometric parameter in the saturated surface area function	0.3/0.81443	
	$\beta_3^{@^o}$: a geometric parameter in the saturated surface area function	0.4/1.92196	
Flux Closure	α^{uc}: a parameter in the closure of e^{uc}	0.1/1.0	
	α_{wg}^u: a parameter in the closure of e_{wg}^u	5/100	
	α^{us}: a parameter in the closure of e^{us}	1	
	α^{oc}: a parameter in the closure of e^{oc}	1.5	
	α^{ro}: a parameter in the closure of e^{ro}	2.5	
	α_1^{os}: a parameter in the closure of e^{os}	10/2000	
	α_2^{os}: a parameter in the closure of e^{os}	5.2/6.2	
	α_3^{os}: a parameter in the closure of e^{os}	2.7	

Hydrological modeling with the REW approach

H. Lee et al.

Title Page

Abstract | Introduction

Conclusions | References

Tables | Figures

◄ | ►|

◄ | ►

Back | Close

Full Screen / Esc

Printer-friendly Version

Interactive Discussion

Table 4. Parameter values for the Weiherbach catchment estimated (a) from the upscaling procedure, (b) by manual calibration of CREW, and (c) by manual calibration of CREW as well as the upscaling procedure.

Group	Description	Parameter value		
		(a)	(b) Nash-Sutcliffe E=0.82	(c) Nash-Sutcliffe E=0.84
Soil	$\beta_1^{|\Psi|}$: bubbling pressure head [m]	0.97	0.21	0.21
	$\beta_2^{|\Psi|}$: inverse of pore size distribution index	0.64	0.25	0.25
	β_1^{K}: u-zone saturated hydraulic conductivity [m/s]	3.0×10^{-6} $(\overline{K_{GEO}})$ $8.0*10^{-7}$ $(\overline{K_{HA}})$ 7.0×10^{-7} $(\overline{K_{AH}})$	8.0×10^{-6}	8.0×10^{-6}
	β_2^{K}: pore disconnectedness index	1.68 $(\overline{K_{GEO}})$ 1.63 $(\overline{K_{HA}})$ 1.49 $(\overline{K_{AH}})$	4.51	4.51
	ε^{u}: u-zone porosity		0.44	0.44
	ε^{s}: s-zone porosity		0.43	0.43
	$\overline{K_s^{s}}$: s-zone saturated hydraulic conductivity [m/s]		3.0×10^{-6}	3.0×10^{-6}
Vegetation	M: canopy density		1.0	1.0
	k_v: ratio of potential rates of transpiration and soil surface evaporation		1.78	1.78
Geographic	$\beta_1^{\varpi^{o}}$: a geometric parameter in the saturated surface area function	0.71	0.06	0.71
	$\beta_2^{\varpi^{o}}$: a geometric parameter in the saturated surface area function	1.79	3.46×10^{-9}	1.79
	$\beta_3^{\varpi^{o}}$: a geometric parameter in the saturated surface area function	0.92	3.73	0.92

Table 4. Continued.

Group	Description	(a)	Parameter value (b) Nash-Sutcliffe E=0.82	(c) Nash-Sutcliffe E=0.84
Hydraulic	n_m^c: Manning roughness coefficient in the c-zone [$m^{-1/3}$ s]		0.07	0.07
	n_m^o: Manning roughness coefficient in the o-zone [$m^{-1/3}$ s]		0.035	0.035
	n_m^r: Manning roughness coefficient in the r-zone [$m^{-1/3}$ s]		0.03	0.03
Flux closure	α^{uc}: a parameter in the closure of e^{uc}		3.51	3.51
	α_{wg}^u : a parameter in the closure of e_{wg}^u		100.0	100.0
	α^{us} : a parameter in the closure of e^{us}		1.32	1.32
	α^{oc} : a parameter in the closure of e^{oc}	1.0	1.0	1.0
	α^{ro} : a parameter in the closure of e^{ro}	1.0	2.5	1.0
	α_1^{os} : a parameter in the closure of e^{os}	0.01	0.45×10^{-4}	0.01
	α_2^{os} : a parameter in the closure of e^{os}	0.60	1.0	0.60
	α_3^{os} : a parameter in the closure of e^{os}	0.31	8.24	0.31
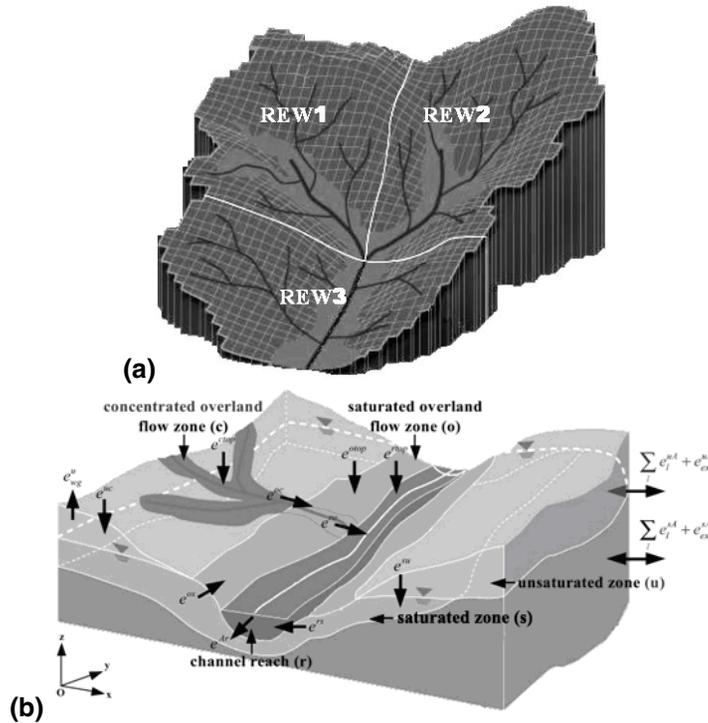
Fig. 1. (a) Catchment discretization into 3 REW units **(b)** Exchanging mass fluxes and subregions making up the spatial domain of a REW after Reggiani et al. (1999, 2000): e^{uc} denotes infiltration, e^u_{wg} evapotranspiration from unsaturated zone, e^{su} recharge or capillary rise, e^{ctop}, e^{otop} and e^{rtop} rainfall or evaporation at c, o and r-zones respectively, e^{oc} concentrated overland flow, e^{ro} saturated overland flow, e^{os} seepage flow, e^{rs} flow from saturated zone to channel, e^{Ar} channel flow at outlet, and $\sum_l e^{uA}_l + e^{uA}_{ext}$ and $\sum_l e^{sA}_l + e^{sA}_{ext}$ mass exchange across mantle segment at u and s-zones, respectively.
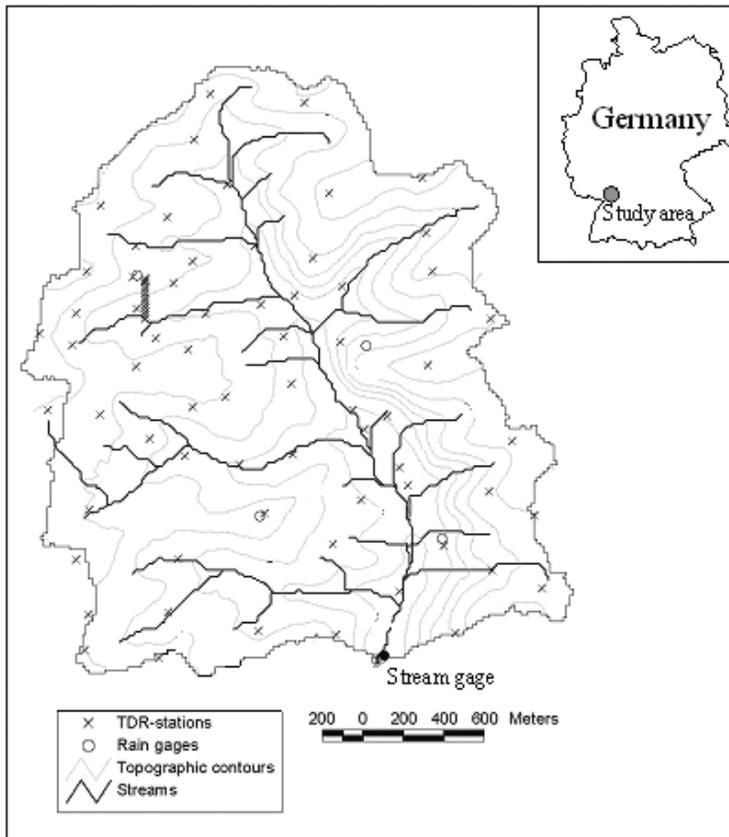
Fig. 2. Observational network of the Weiherbach catchment, after Zehe et al. (2005a): soil moisture was measured at 61 TDR stations at weekly intervals (crosses). Topographic contour interval is 10 m.

EGU
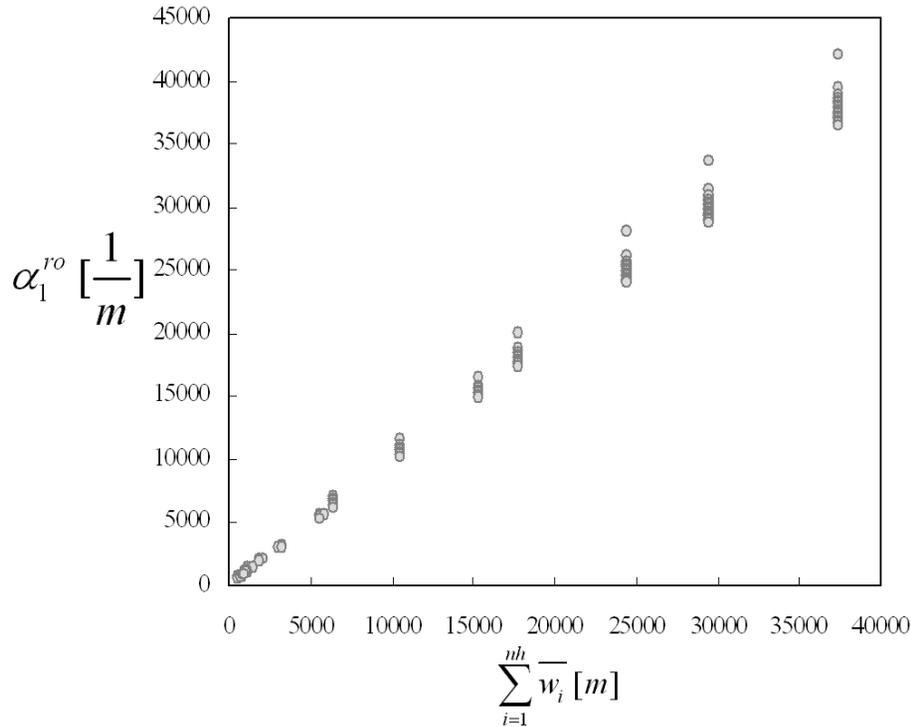
Fig. 3. Dependence test of parameter α_1^{ro} to hillslope width.

Title Page

Abstract | Introduction

Conclusions | References

Tables | Figures

◄◄ | ►►

◄ | ►

Back | Close

Full Screen / Esc

Printer-friendly Version

Interactive Discussion

EGU
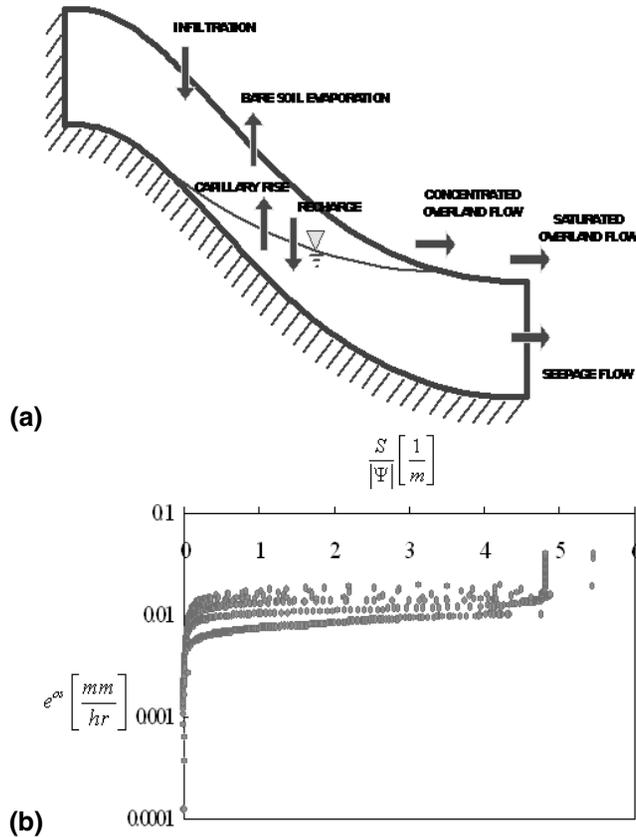
Fig. 4. (a) Hillslope setting for developing closure relation for seepage flux, using CATFLOW simulation; and **(b)** the best candidate for the seepage flux closure relation.
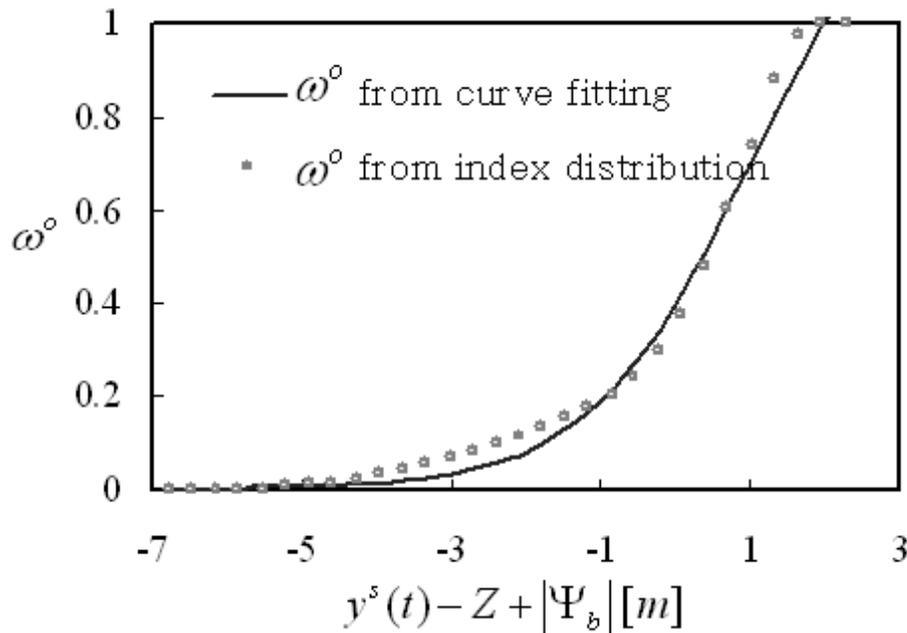
Fig. 5. Geometric relationship for saturated area fraction as a function of averaged thickness of saturated zone.

EGU
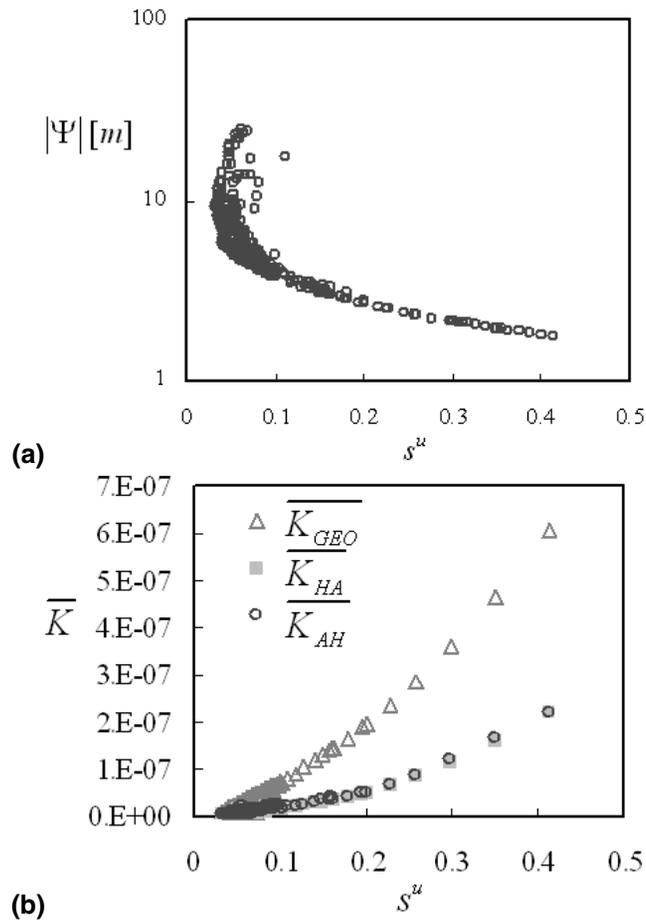
Fig. 6. Catchment scale **(a)** water retention curve, and **(b)** hydraulic conductivity curve, based on CATFLOW simulations.

HESSD

3, 1667–1743, 2006

Hydrological modeling with the REW approach

H. Lee et al.

Title Page

Abstract | Introduction

Conclusions | References

Tables | Figures

◄◄ | ►►

◄ | ►

Back | Close

Full Screen / Esc

Printer-friendly Version

Interactive Discussion

EGU
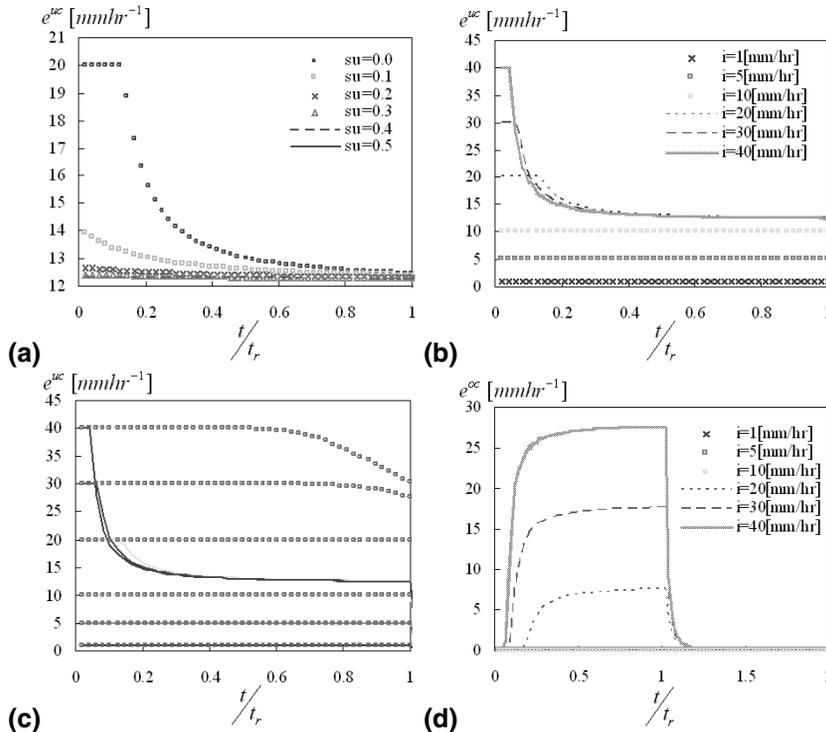
Fig. 7. Sensitivity analysis on closure relation for infiltration and concentrated overland flow **(a)** the effect of antecedent moisture content on the closure relation for infiltration process: silty loam **(b)** climate effect on the closure relation for infiltration process: silty loam **(c)** the effect of different soil on the closure relation for infiltration rate: solid line for silty loam, circle for sand **(d)** climate effect on the closure relation for concentrated overland flow: silty loam.

Hydrological modeling with the REW approach

H. Lee et al.

Title Page

Abstract | Introduction

Conclusions | References

Tables | Figures

|◄ | ►|

◄ | ►

Back | Close

Full Screen / Esc

Printer-friendly Version

Interactive Discussion

EGU
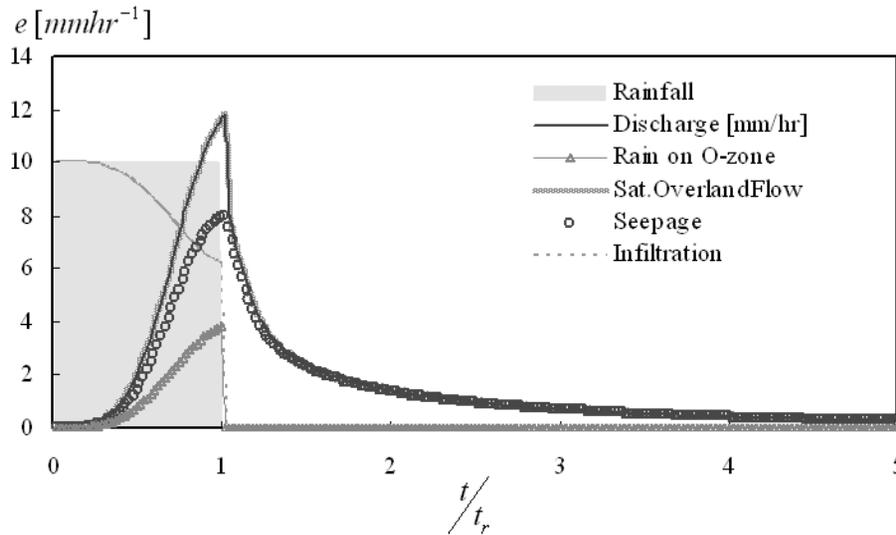
Fig. 8. Saturated overland flow and discharge at the channel outlet as the integrated response of all processes happening in the catchment.
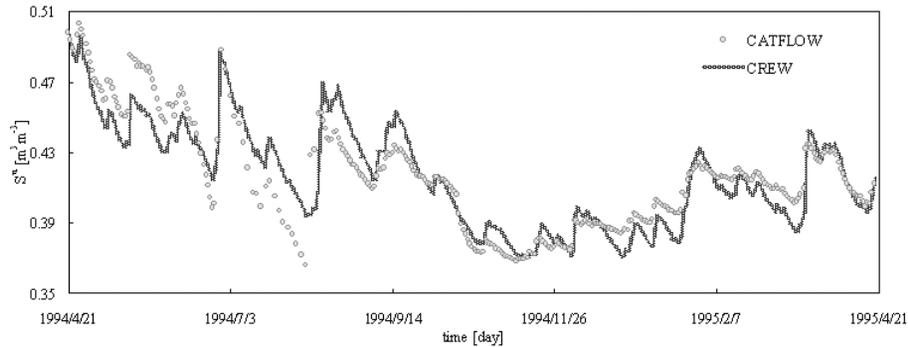
Fig. 9. Comparison of catchment scale saturation degree in the unsaturated zone, s^u, simulated from CATFLOW and CREW.

EGU
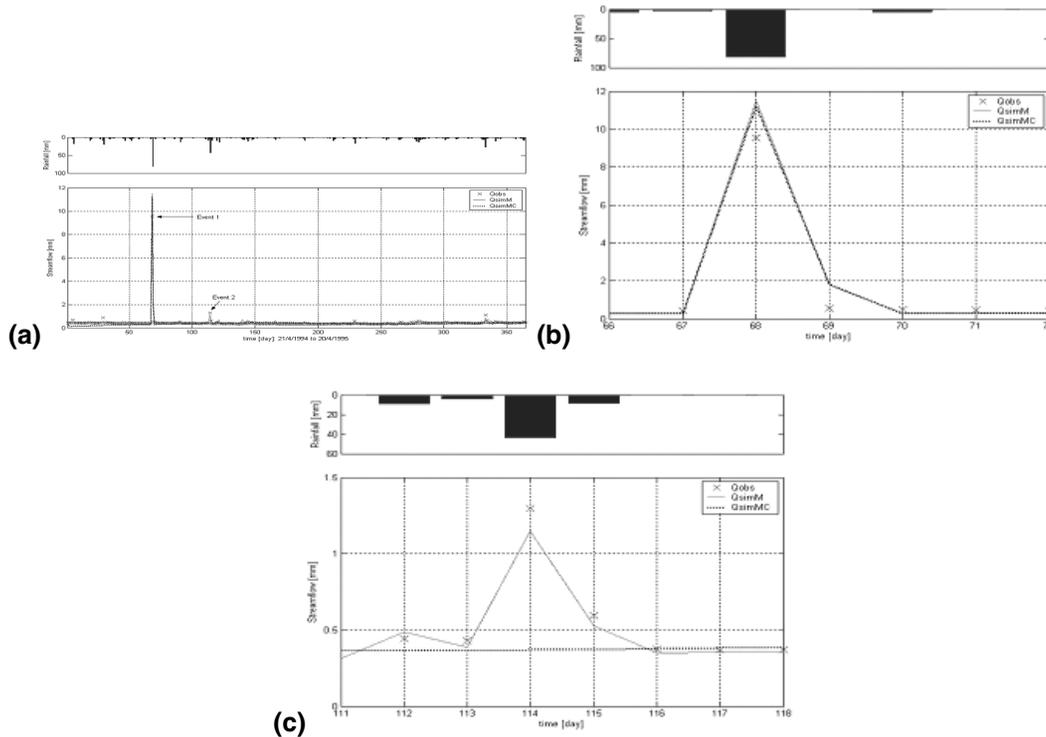
Fig. 10. Comparison of observed streamflows with those simulated by CREW at the daily time scale where Qobs, QsimM and QsimMC denote the observed hydrograph, simulated hydrograph with manually calibrated parameter values, and simulated hydrograph with both closure parameters as well as manually calibrated ones, respectively: daily rainfall and streamflow time series from Weiherbach catchment **(a)** from 21 April 1994 to 20 April 1995, **(b)** for event 1, and **(c)** for event 2, and runoff contribution of different hydrologic processes for **(d)** event 1, and **(e)** event 2 where IE, SE, SS, and Q denote infiltration excess, saturation excess overland flow, subsurface flow, and streamflow, respectively.

EGU

HESSD

3, 1667–1743, 2006

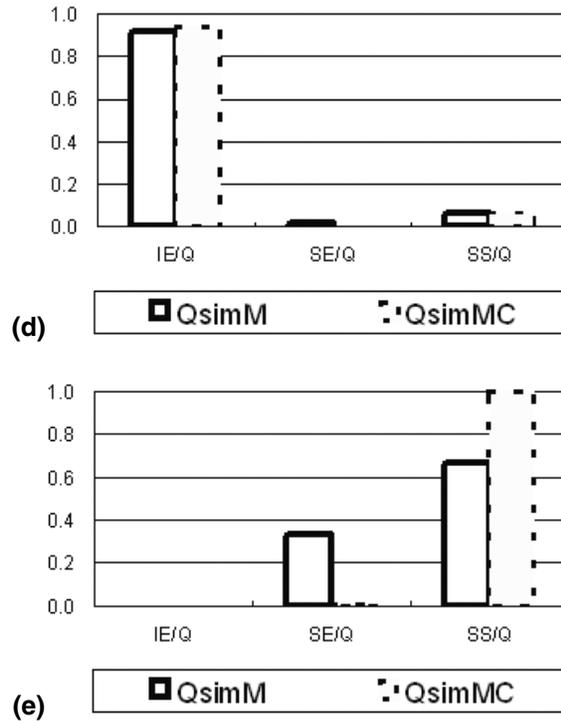**Hydrological modeling with the REW approach**

H. Lee et al.

Title Page

Abstract | Introduction

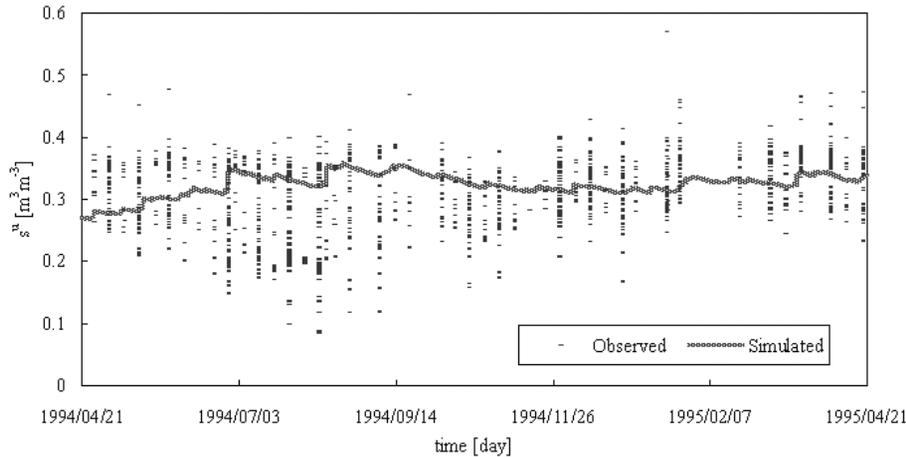Conclusions | References

Tables | Figures

◄ | ►

◄ | ►

Back | Close

Full Screen / Esc

Printer-friendly Version

Interactive Discussion

EGU

(d)

(e)

Fig. 10. Continued.

Fig. 11. Comparison of 60 cm depth averaged measured surface soil moisture content with saturation degree in the unsaturated zone, s^u, simulated by CREW.

EGU